RESEARCH ARTICLE

Neutrophil infiltration regulates clock-gene expression to organize daily hepatic metabolism

María Crespo[1†], Barbara Gonzalez-Teran[1†], Ivana Nikolic[1], Alfonso Mora[1], Cintia Folgueira[1], Elena Rodríguez[1], Luis Leiva-Vega[1], Aránzazu Pintor-Chocano[1], Macarena Fernández-Chacón[1], Irene Ruiz-Garrido[1], Beatriz Cicuéndez[1], Antonia Tomás-Loba[1], Noelia A-Gonzalez[1], Ainoa Caballero-Molano[1], Daniel Beiroa[2,3], Lourdes Hernández-Cosido[4], Jorge L Torres[5], Norman J Kennedy[6], Roger J Davis[6], Rui Benedito[1], Miguel Marcos[5], Ruben Nogueiras[2,3], Andrés Hidalgo[1], Nuria Matesanz[1]*, Magdalena Leiva[1†]*, Guadalupe Sabio[1]*

[1]Centro Nacional de Investigaciones Cardiovasculares Carlos (CNIC), Madrid, Spain; [2]CIBER Fisiopatología de la Obesidad y Nutrición (CIBERobn), Santiago de Compostela, Spain; [3]CIMUS, University of Santiago de Compostela-Instituto de Investigación Sanitaria, Santiago de Compostela, Spain; [4]Department of General Surgery, University Hospital of Salamanca-IBSAL, Department of Surgery, University of Salamanca, Salamanca, Spain; [5]Department of Internal Medicine, University Hospital of Salamanca-IBSAL, Department of Medicine, University of Salamanca, Salamanca, Spain; [6]Howard Hughes Medical Institute and Program in Molecular Medicine, University of Massachusetts Medical School, Worcester, United States

***For correspondence:**
nuria.matesanz@cnic.es (NM);
magdalena.leiva@cnic.es (ML);
gsabio@cnic.es (GS)

[†]These authors contributed equally to this work

Competing interests: The authors declare that no competing interests exist.

Funding: See page 16

Received: 23 May 2020
Accepted: 04 November 2020
Published: 08 December 2020

Reviewing editor: Florent Ginhoux, Agency for Science Technology and Research, Singapore

Abstract Liver metabolism follows diurnal fluctuations through the modulation of molecular clock genes. Disruption of this molecular clock can result in metabolic disease but its potential regulation by immune cells remains unexplored. Here, we demonstrated that in steady state, neutrophils infiltrated the mouse liver following a circadian pattern and regulated hepatocyte clock-genes by neutrophil elastase (NE) secretion. NE signals through c-Jun NH2-terminal kinase (JNK) inhibiting fibroblast growth factor 21 (FGF21) and activating *Bmal1* expression in the hepatocyte. Interestingly, mice with neutropenia, defective neutrophil infiltration or lacking elastase were protected against steatosis correlating with lower JNK activation, reduced *Bmal1* and increased FGF21 expression, together with decreased lipogenesis in the liver. Lastly, using a cohort of human samples we found a direct correlation between JNK activation, NE levels and *Bmal1* expression in the liver. This study demonstrates that neutrophils contribute to the maintenance of daily hepatic homeostasis through the regulation of the NE/JNK/*Bmal1* axis.

Introduction

Circadian rhythms regulate several biological processes through internal molecular mechanisms (***Dibner et al., 2010***) and the chronic perturbation of circadian rhythms is associated with the appearance of metabolic syndrome (***Kolla and Auger, 2011***). This homeostasis is closely dependent on the circadian system in the liver, which shows rhythmic expression of enzymes associated with glucose and lipid metabolism (***Haus and Halberg, 1966***; ***North et al., 1981***; ***Tahara and Shibata, 2016***). Moreover, mice with mutations in clock genes encoding nuclear receptors have impaired glucose and lipid metabolism and are susceptible to diet-induced obesity and metabolic dysfunction,

eLife digest Every day, the body's biological processes work to an internal clock known as the circadian rhythm. This rhythm is controlled by 'clock genes' that are switched on or off by daily physical and environmental cues, such as changes in light levels. These daily rhythms are very finely tuned, and disturbances can lead to serious health problems, such as diabetes or high blood pressure.

The ability of the body to cycle through the circadian rhythm each day is heavily influenced by the clock of one key organ: the liver. This organ plays a critical role in converting food and drink into energy. There is evidence that neutrophils – white blood cells that protect the body by being the first response to inflammation – can influence how the liver performs its role in obese people, by for example, releasing a protein called elastase. Additionally, the levels of neutrophils circulating in the blood change following a daily pattern. Crespo, González-Terán et al. wondered whether neutrophils enter the liver at specific times of the day to control liver's daily rhythm.

Crespo, González-Terán et al. revealed that neutrophils visit the liver in a pattern that peaks when it gets light and dips when it gets dark by counting the number of neutrophils in the livers of mice at different times of the day. During these visits, neutrophils secreted elastase, which activated a protein called JNK in the cells of the mice's liver. This subsequently blocked the activity of another protein, FGF21, which led to the activation of the genes that allow cells to make fat molecules for storage. JNK activation also switched on the clock gene, *Bmal1*, ultimately causing fat to build up in the mice's liver. Crespo, González-Terán et al. also found that, in samples from human livers, the levels of elastase, the activity of JNK, and whether the *Bmal1* gene was switched on were tightly linked. This suggests that neutrophils may be controlling the liver's rhythm in humans the same way they do in mice.

Overall, this research shows that neutrophils can control and reset the liver's daily rhythm using a precisely co-ordinated series of molecular changes. These insights into the liver's molecular clock suggest that elastase, JNK and *Bmal1* may represent new therapeutic targets for drugs or smart medicines to treat metabolic diseases such as diabetes or high blood pressure.

consistent with the idea that these genes control hepatic metabolic homeostasis (**Delezie et al., 2012**; **Kudo et al., 2008**; **Lamia et al., 2008**; **Rey et al., 2011**; **Tong and Yin, 2013**; **Turek et al., 2005**; **Yang et al., 2006**). Besides, recent reports have shown that hepatic physiology follows a diurnal rhythm driven by clock genes, with expression of proteins involved in fatty acid synthesis higher in the morning while those controlling fatty acid oxidation are higher at sunset (**Toledo et al., 2018**; **Zhou et al., 2015**).

Blood leukocyte levels also oscillate diurnally, as does the release of hematopoietic stem cells and progenitor cells from the bone marrow (BM) (**Haus and Smolensky, 1999**; **Lucas et al., 2008**; **Méndez-Ferrer et al., 2008**) and their recruitment into tissues (**Adrover et al., 2019**; **He et al., 2018**; **Scheiermann et al., 2012**). Oscillatory expression of clock genes in peripheral tissues is largely tuned by the suprachiasmatic nucleus (**Dibner et al., 2010**; **Druzd and Scheiermann, 2013**; **Huang et al., 2011**; **Reppert and Weaver, 2002**); however, the potential regulation of daily rhythms of specific tissues by immune cells remains largely unexplored, both in steady state and during inflammation. Although the molecular mechanisms linking circadian rhythms and metabolic disease are largely unknown, several studies have demonstrated a strong association between leukocyte activation and metabolic diseases (**McNelis and Olefsky, 2014**). A prime example is the BM, where engulfment of infiltrating neutrophils by tissue-resident macrophages modulates the hematopoietic niche (**Casanova-Acebes et al., 2013**).

The circadian clock is dysregulated by obesity (**Kohsaka et al., 2007**; **Xu et al., 2014**), and recent studies suggest that liver leukocyte recruitment and migration show a circadian rhythm (**Scheiermann et al., 2012**; **Solt et al., 2012**) whose alteration can result in steatosis (**Solt et al., 2012**; **Xu et al., 2014**). Neutrophils are key factors in steatosis development (**González-Terán et al., 2016**; **Keller et al., 2009**; **Mansuy-Aubert et al., 2013**; **Nathan, 2006**) and show diurnal oscillations in their recruitment and migration to multiple tissues (**Scheiermann et al., 2012**; **Solt et al., 2012**). Here, we demonstrate that circadian neutrophil infiltration into the liver controls the expression of

clock genes through the regulation of c-Jun NH2-terminal kinase (JNK) and the hepatokine fibroblast growth factor 21 (FGF21), driving adaptation to daily metabolic rhythm.

Results

Rhythmic neutrophil infiltration into the liver modulates the expression of hepatic clock genes

Virtually all cell types have an internal clock that controls their rhythmicity through the periodic expression of clock genes (**Robles et al., 2014**; **Tahara and Shibata, 2016**). However, it is unknown how these multiple cell rhythms are integrated. The liver is an essential metabolic organ that controls body glucose and lipid homeostasis (**Manieri and Sabio, 2015**), and neutrophil infiltration alters its function (**González-Terán et al., 2016**). We hypothesized that the metabolic cycles in the liver might be entrained by rhythmic neutrophil infiltration. To test this, we harvested liver, BM, and blood from C57BL6J mice at 4 hr intervals over a 24 hr period. Liver neutrophil infiltration showed a clear diurnal pattern, with a peak at ZT2, coinciding with liver-driven lipogenesis in mice (**Zhou et al., 2015**), and a nadir during the night, at ZT14 (**Figure 1A**), correlating with lipolysis (**Zhou et al., 2015**). These oscillations corresponded directly to changes in neutrophil numbers in blood (**Figure 1—figure supplement 1A**), suggesting that liver infiltration might result from higher neutrophil migration to the liver. We first confirmed that neutrophils were infiltrated in the liver using 3D microscopy. According to published data (**Casanova-Acebes et al., 2018**), infiltrated neutrophils presented an intrasinusoidal distribution in the liver, different to that observed in the Kupffer cells population (**Figure 1B** and **Figure 1—figure supplement 1B**). Then we evaluated whether myeloid chemokines could be involved in circadian neutrophil recruitment into the liver. Analysis of liver lysates indicated that the expression of the hepatocyte-derived neutrophil chemoattractant *Cxcl1* (**Su et al., 2018**) was higher at ZT2 than a ZT14. Moreover, mRNA of *Cxcl1* in liver samples showed the same oscillation pattern than infiltrated neutrophils, suggesting that this chemokine may be important in the regulation of the neutrophil diurnal cycle (**Figure 1—figure supplement 1C**).

The infiltration pattern correlated with liver expression levels of the clock-gene *Bmal1*, peaking at ZT2 and bottoming at ZT14 (**Figure 1C**). Infiltration also correlated inversely with the expression of *Nr1d2* (encoding Rev-erb β), *Per2*, and *Cry2* (**Figure 1C**), which are important proteins in the control of circadian rhythms (**Reppert and Weaver, 2002**), consistent with the feedback loop that controls their expression. *Bmal1* is thought to induce lipogenesis (**Zhang et al., 2014**), whereas *Nr1d2* controls lipid metabolism and its reduced expression promotes lipogenesis and steatosis (**Delezie et al., 2012**; **Solt et al., 2012**). In agreement with these studies, liver triglycerides were higher at ZT2 than at ZT14 (**Figure 1D**).

Our results show a correlation between neutrophil infiltration, hepatocyte *Bmal1* expression, and lipid metabolism regulation, raising the possibility that neutrophils signal to hepatocytes to modulate the expression of circadian genes. Exposure of mouse hepatocytes *in vitro* to freshly isolated neutrophils increased hepatocyte expression of the clock genes *Bmal1* and *Clock*. In contrast, no effect was observed upon exposure to T or B lymphocytes, or macrophages, suggesting the existence of a neutrophil-to-hepatocyte communication that controls hepatocyte clock-gene expression (**Figure 1E** and **Figure 1—figure supplement 1D**).

We then investigated whether neutrophil elastase (NE), a proteolytic enzyme reported to regulate liver metabolism, could regulate hepatocyte clock genes (**Mansuy-Aubert et al., 2013**; **Talukdar et al., 2012**). Exposure to elastase reproduced the same increase in hepatocyte *Bmal1* and *Clock* expression in contrast with another protease that did not affect *Bmal1* expression (**Figure 1F** and **Figure 1—figure supplement 1D**).

Next, neutrophil-mediated regulation of liver clock-gene expression *in vivo* was investigated using a previously characterized genetic model of neutrophil deficiency (**Dzhagalov et al., 2007**; **Steimer et al., 2009**; **Figure 1—figure supplement 1E,F** and **Figure 1—figure supplement 2A–C**). Low hepatic neutrophil infiltration in neutropenic mice correlated with reduced expression of *Bmal1* and *Clock* (**Figure 1G**) and increased expression of *Cry2* and *Per2* at ZT2 (**Figure 1G**). These changes in clock-gene expression were accompanied by lower liver triglyceride levels (**Figure 1H**). Furthermore, lack of neutrophils perturbed the diurnal rhythmicity in *Bmal1*, *Clock*, and *Per2* expression in the liver without affecting clock genes in other organs such as the lung, in which there is no

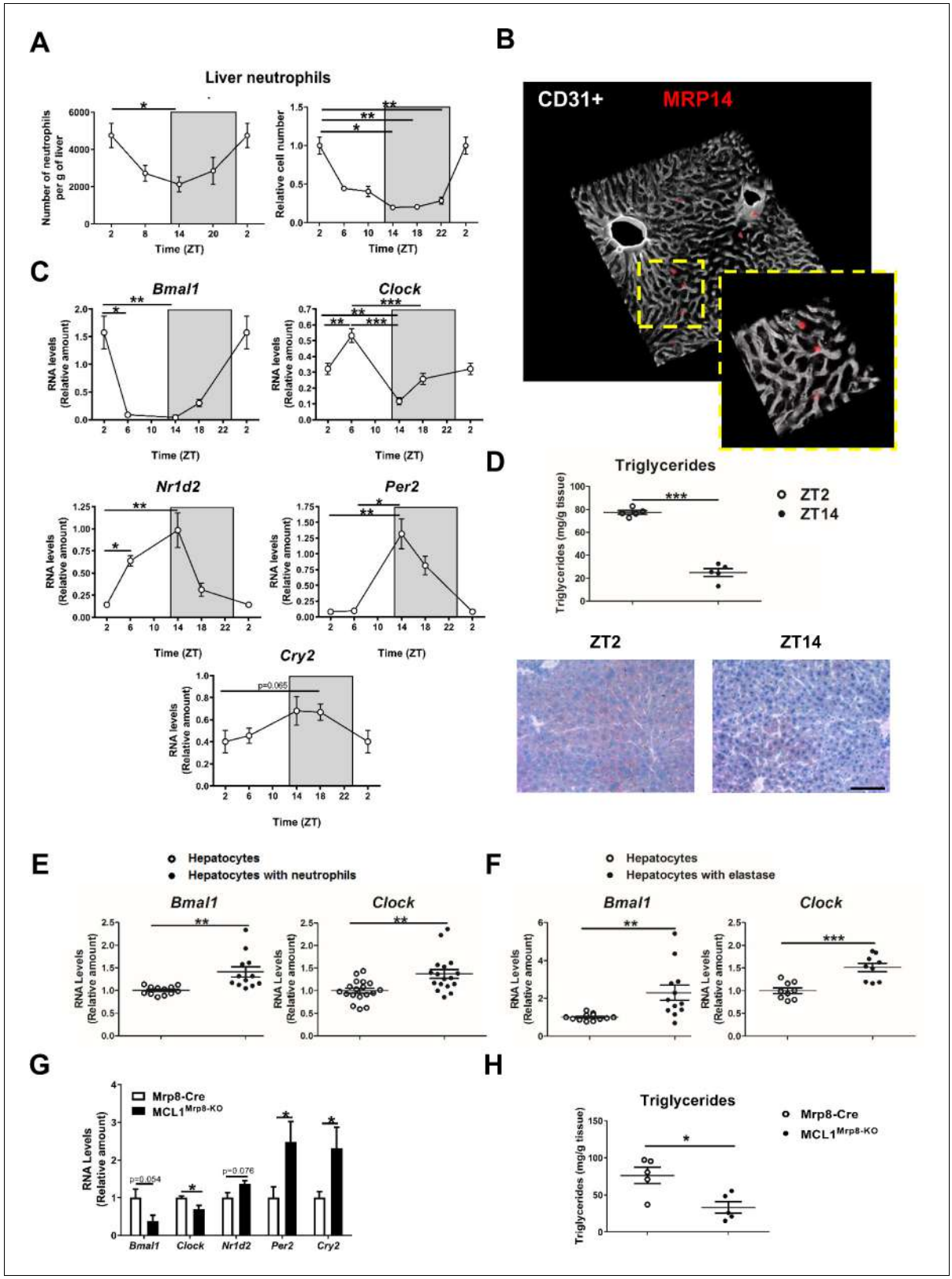

Figure 1. Neutrophil infiltration into the liver controls hepatic clock-gene expression. (**A**) Flow cytometry analysis of the CD11b^{+}Ly6G^{+} liver myeloid subset, isolated from C57BL6J mice at the indicated ZTs. Left, CD11b^{+}Ly6G^{+} liver myeloid subset analyzed at 6 hr intervals and normalized by the tissue weight. Right, percentage of CD11b^{+}Ly6G^{+} population analyzed at 4 hr intervals and normalized to ZT2 (n = 5). (**B**) Representative 3-D image of liver section showing the distribution on infiltrated neutrophils. Livers were stained with anti-S100A9 (Mrp14) (red) and vessels were stained with anti-

Figure 1 continued on next page

Figure 1 continued

CD31 and anti-endomucin (grey). Sizes of the liver sections are 510 x 510 x 28 µm and 160 x 160 x 28 µm, respectively. (**C**) qRT-PCR analysis of circadian clock-gene and nuclear-receptor mRNA expression in livers from C57BL6J mice at the indicated ZTs (n = 5). (**D**) Liver triglycerides and oil-red-stained liver sections prepared from C57BL6J mice at ZT2 and ZT14. Scale bar, 50 µm (n = 5). (**E**) qRT-PCR analysis of clock-gene mRNA in hepatocyte cultures exposed to freshly isolated FMLP-activated neutrophils (n = 4-6 wells of 3 independent experiments). (**F**) qRT-PCR analysis of clock-gene mRNA in hepatocyte cultures treated with 5 nM elastase (n = 3-4 wells of 3 independent experiments). (**G**) qRT-PCR analysis of clock-gene and nuclear-receptor mRNA expression in livers from control mice (Mrp8-Cre) and neutropenic mice ($MCL1^{Mrp8\text{-}KO}$) sacrificed at ZT2 (n = 5). (**H**) Hepatic triglycerides detected in livers from control mice (Mrp8-Cre) and neutropenic mice ($MCL1^{Mrp8\text{-}KO}$) at ZT2 (n = 5). Data are means ± SEM from at least 2 independent experiments. *p<0.05; **p<0.01; ***p<0.005 (A, left panel) One-way ANOVA with Tukey's post hoc test. (A, right panel) Kruskal-Wallis test with Dunn's post hoc test. (**C**) One-way ANOVA with Tukey's post hoc test or Kruskal-Wallis test with Dunn's post hoc test. (D to H) *t-test* or Welch's test. ZT2 point is double plotted to facilitate viewing.

The online version of this article includes the following source data and figure supplement(s) for figure 1:

Source data 1. Raw data and statistical test.
Figure supplement 1. Neutrophils follow a circadian rhythm.
Figure supplement 1—source data 1. Raw data and statistical test.
Figure supplement 2. Neutrophil deficiency alters clock-gene expression.
Figure supplement 2—source data 1. Raw data and statistical test.

correlation between the peak of neutrophil infiltration and *Bmal1* expression (***Figure 1—figure supplement 2D,E***). Our results thus indicate that neutrophils might specifically control the expression of hepatocyte circadian clock genes in steady state.

Disruption of daily neutrophil infiltration in the liver affects hepatocyte molecular clock and metabolism

Chronic jet lag alters liver circadian genes and disrupts liver metabolism (***Kettner et al., 2016***). Analysis of a mouse model of jet lag revealed complete disruption of the circadian liver neutrophil infiltration with increased hepatic neutrophil infiltration even at ZT14 (***Figure 2A***). Abolition of rhythmic neutrophil hepatic infiltration under jet lag correlated with increased steatosis and high levels of liver triglycerides (***Figure 2B***). To evaluate whether the metabolic effect of circadian perturbation was caused by the increased neutrophil infiltration, we exposed neutropenic and control mice to the jet lag protocol (***Figure 2—figure supplement 1A,B***). Jet lag-induced steatosis was less severe in neutropenic mice (***Figure 2C***), and disruption of diurnal liver expression of *Bmal1* detected in control jet-lagged mice was partially ablated in neutropenic mice (***Figure 2D***). Similar results were also observed in mice with impaired neutrophil migration such as $Cxcr2^{MRP8\text{-}KO}$ BM transplanted mice (***Eash et al., 2010***; ***Mei et al., 2012***) and $p38\gamma/\delta^{Lyzs\text{-}KO}$ mice (***González-Terán et al., 2016***). In both models, the reduction of neutrophil infiltration correlated with decreased levels of liver *Bmal1* expression and protection from jet lag-induced steatosis (***Figure 2—figure supplement 1C–G***). These results are consistent with the role of neutrophils in the control of liver clock genes.

Inflammation plays a key role in the pathogenesis of non-alcoholic fatty liver disease (***Tiniakos et al., 2010***) and the development of hepatic steatosis is associated with increased liver infiltration by myeloid cells, particularly neutrophils (***González-Terán et al., 2016***; ***Mansuy-Aubert et al., 2013***; ***Talukdar et al., 2012***; ***Tiniakos et al., 2010***). Two widely used mouse models of hepatic steatosis, high-fat diet (HFD) and methionine-choline-deficient (MCD) diet, increased liver neutrophil infiltration in WT mice at ZT2, ZT14, and ZT18 (***Figure 2E,F***). Consistent with a neutrophil-to-hepatocyte communication in the regulation of hepatocyte clock genes, the MCD diet enhanced *Bmal1* expression and inhibited *Cry2* and *Per2* expression in control mice, but not in neutropenic mice at ZT2 (***Figure 2G***). Altered liver clock-gene regulation in neutropenic mice was associated with protection against steatosis and lower liver triglycerides (***Figure 2H***). To confirm the role of neutrophils in modulating liver clock genes, we depleted neutrophils by injecting anti-Ly6G antibody into MCD diet-fed mice (***González-Terán et al., 2016***). Anti-Ly6G administration for 7 days reduced circulating neutrophil levels without affecting monocytes (***Figure 2—figure supplement 2A,B***), and treatment for 21 days markedly decreased hepatic diurnal *Bmal1* and *Clock* expression, increased expression of *Cry2*, and *Per2* (***Figure 2—figure supplement 2C***) and consequently reduced steatosis (***González-Terán et al., 2016***).

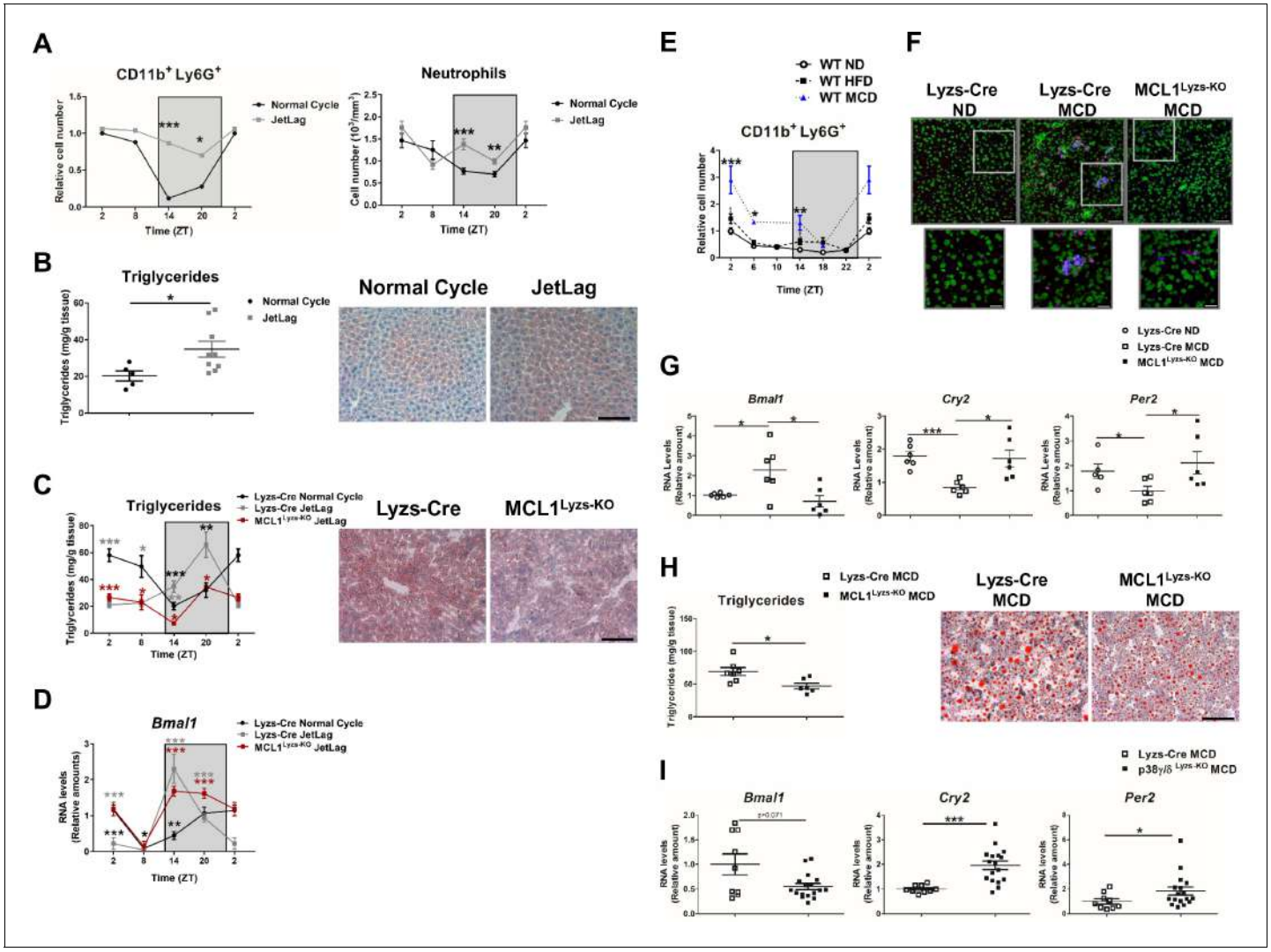

Figure 2. Increased hepatic neutrophil infiltration alters clock-genes expression and augments triglyceride content in the liver. (**A–D**) Control (Lyzs-Cre) (**A–B**) and control and neutropenic (MCL1$^{Lyzs\text{-}KO}$) mice (**C–D**) were housed for 3 weeks with a normal 12 hr: 12 hr light/dark cycle (Normal Cycle) or with the dark period extended by 12 hr every 5 days (JetLag). Samples were obtained at the indicated ZTs. (**A**) Left, flow cytometry analysis of the CD11b$^+$Ly6G$^+$ liver myeloid subset. Data represents the percentage CD11b$^+$Ly6G$^+$ normalized to Normal Cycle ZT2. Right, circulating neutrophils in whole blood. (n = 5-8). (**B**) Liver triglycerides and representative oil-red-stained liver sections at ZT14. Scale bar, 50 µm (n = 9-10). (**C**) Hepatic triglyceride content analyzed at 6 hr intervals, and representative oil-red-stained liver sections at ZT14. Scale bar, 50 µm (n = 4-6). (**D**) qRT-PCR analysis of *Bmal1* mRNA in livers. (n = 5-8). (**E**) Flow cytometry analysis of the CD11b$^+$Ly6G$^+$ liver myeloid subset isolated at 6 hr intervals from C57BL6J mice fed a ND, a HFD (8 weeks) or a MCD (3 weeks). The chart shows the CD11b$^+$Ly6G$^+$ population as a percentage of the total intrahepatic CD11b$^+$ leukocyte population normalized to ND group at ZT2 (n = 5 to 10). (**F–I**) Control mice (Lyzs-Cre) and neutropenic mice (MCL1$^{Lyzs\text{-}KO}$) or p38γ/δ$^{Lyzs\text{-}KO}$ were fed a ND or the MCD diet for 3 weeks and sacrificed at ZT2. (**F**) Representative images of the infiltration of neutrophils in the liver stained with anti-Mrp14 (blue) and anti-NE (red); nuclei with Sytox Green. Scale bar, 50 µm (Top) and 25 µm (Bottom). (**G**) qRT-PCR analysis of clock-gene expression in livers (n = 6). (**H**) Liver triglycerides and representative oil-red-stained liver sections. Scale bar, 50 µm (n = 7-6). (**I**) qRT-PCR analysis of clock genes in livers at ZT2 (n = 9-17). Data are means ± SEM from at least two independent experiments. *p<0.05; **p<0.01; ***p<0.005 (A to D) *t-test* or Welch's test. (**E**) Two-way ANOVA with Fisher's post hoc test; p<0.05 ND vs HFD; p<0.0001 ND vs MCD. *p<0.05; ***p<0.005 (G to I) *t-test* or Welch's test. ZT2 point is double plotted to facilitate viewing.

The online version of this article includes the following source data and figure supplement(s) for figure 2:

Source data 1. Raw data and statistical test.
Figure supplement 1. Defective neutrophil migration to the liver alters hepatic clock- gene expression and triglyceride content.
Figure supplement 1—source data 1. Raw data and statistical test.
Figure supplement 2. Neutrophil depletion alters hepatic clock-gene expression.
Figure supplement 2—source data 1. Raw data and statistical test.
Figure supplement 2—source data 2. Raw data and statistical test.

To further support the role of neutrophil liver infiltration in the regulation of liver clock genes and hepatic lipogenesis during diet-induced steatosis, we leveraged a mouse model (p38γ/δ$^{Lyzs\text{-}KO}$) that exhibits deficient neutrophil migration and subsequently, reduced liver neutrophil infiltration after MCD diet (**González-Terán et al., 2016**). Compared with diet-matched control (Lyzs-Cre) mice, MCD-diet-fed p38γ/δ$^{Lyzs\text{-}KO}$ mice showed hepatic down-regulation of *Bmal1*, which was associated with higher expression of *Cry2*, and *Per2* (**Figure 2I**). These results suggest that the reduced neutrophil infiltration in mice lacking myeloid p38γ/δ expression is responsible for the altered expression of circadian clock genes. Overall, these findings strongly support that neutrophil infiltration modulates clock-gene expression in the liver, with downstream effects on liver metabolism.

Regulation of daily hepatic metabolism by neutrophils through JNK-FGF21 axis

It has been suggested that JNK activation in the liver may be regulated in a circadian manner with a peak at noon (**Robles et al., 2014**). To evaluate whether neutrophils might mediate this diurnal regulation of JNK, we analyzed JNK activation in neutropenic mice. Lack of neutrophils was associated with lower liver expression and activation of JNK, lower activation of the JNK downstream effector c-Jun, and lower expression of acetyl-CoA carboxylase (*Acaca*), a key enzyme in metabolic regulation (acetyl-CoA carboxylase; ACC) that mediates inhibition of beta-oxidation and activation of lipid biosynthesis (**Figure 3A** and **Figure 3—figure supplement 1A**). Similar results were found in p38γ/δ$^{Lyzs\text{-}KO}$ mice, in which reduced liver neutrophil infiltration was associated with decreased JNK phosphorylation and ACC protein levels (**Figure 3B** and **Figure 3—figure supplement 1B**). Moreover, neutrophil-treated hepatocytes showed increased JNK activation together with increased levels of ACC expression (**Figure 3—figure supplement 1C**). NE represents a potential mediator of this neutrophil function because elastase-treated hepatocytes also showed higher JNK activation, suggesting that this protease modulates the expression of the clock genes through the JNK signaling pathways (**Figure 3C** and **Figure 3—figure supplement 1D**). This JNK activation was accompanied by increased *Bmal1* expression (**Figure 3D**), indicating that neutrophils altered liver clock-gene expression through the elastase-JNK pathway.

Our results suggest that neutrophil-mediated JNK activation might modulate hepatocyte clock genes and metabolism through the regulation of ACC. Supporting this hypothesis, specific JNK depletion in hepatocytes downregulated *Bmal1*, *Clock*, and *Acaca* compared to Alb-Cre (**Figure 3E** and **Figure 3—figure supplement 1E**). According to these results, JNK inhibition reduced the expression of *Bmal1*, *Clock* and *Acaca* in WT liver but not in neutropenic mice (**Figure 3—figure supplement 1F,G**). These data strongly suggest that JNK activation caused by neutrophil infiltration modulates clock genes and daily metabolism in hepatocytes.

JNK is an important modulator of the expression of the hepatokine circadian regulator FGF21 (**Vernia et al., 2014**), which controls glucose and lipid metabolism (**Fisher and Maratos-Flier, 2013**; **Li et al., 2013**; **Potthoff et al., 2012**). Mice lacking JNK in hepatocytes had higher FGF21 mRNA expression (**Figure 3E**). In concordance with high JNK activation, FGF21 expression was reduced in neutrophil-exposed hepatocytes (**Figure 3—figure supplement 1H**). Moreover, neutropenic and p38γ/δ$^{Lyzs\text{-}KO}$ mice showed increased FGF21 expression (**Figure 3F** and **Figure 3—figure supplement 1I,J**), which was consistent with the reduced hepatocyte JNK activation in these mice.

To further define the role of FGF21 in the neutrophil-mediated regulation of liver metabolism, we suppressed FGF21 expression using two independent lentiviral shRNA vectors (**Figure 3G** and **Figure 3—figure supplement 1K**). The protection of p38γ/δ$^{Lyzs\text{-}KO}$ mice against MCD-diet-induced alterations was abrogated by shFGF21 and these mice developed steatosis with an elevated hepatic triglyceride content (**Figure 3H,I**). These data further supported the idea that neutrophil infiltration controls liver metabolism through the regulation of FGF21 expression.

Neutrophil elastase deficiency affects the expression patterns of clock genes and lipid metabolism

To formally confirm the involvement of NE in circadian clock alteration, we first evaluated the diurnal oscillation of NE levels in liver from WT mice fed a normal diet (ND). According to infiltration pattern of neutrophils in the liver (**Figure 1A**), we found higher NE levels at ZT2 than at ZT14. (**Figure 4A**). Next, circadian clock-gene expression in NE$^{-/-}$ mice revealed lower *Bmal1* and elevated *Per2* and

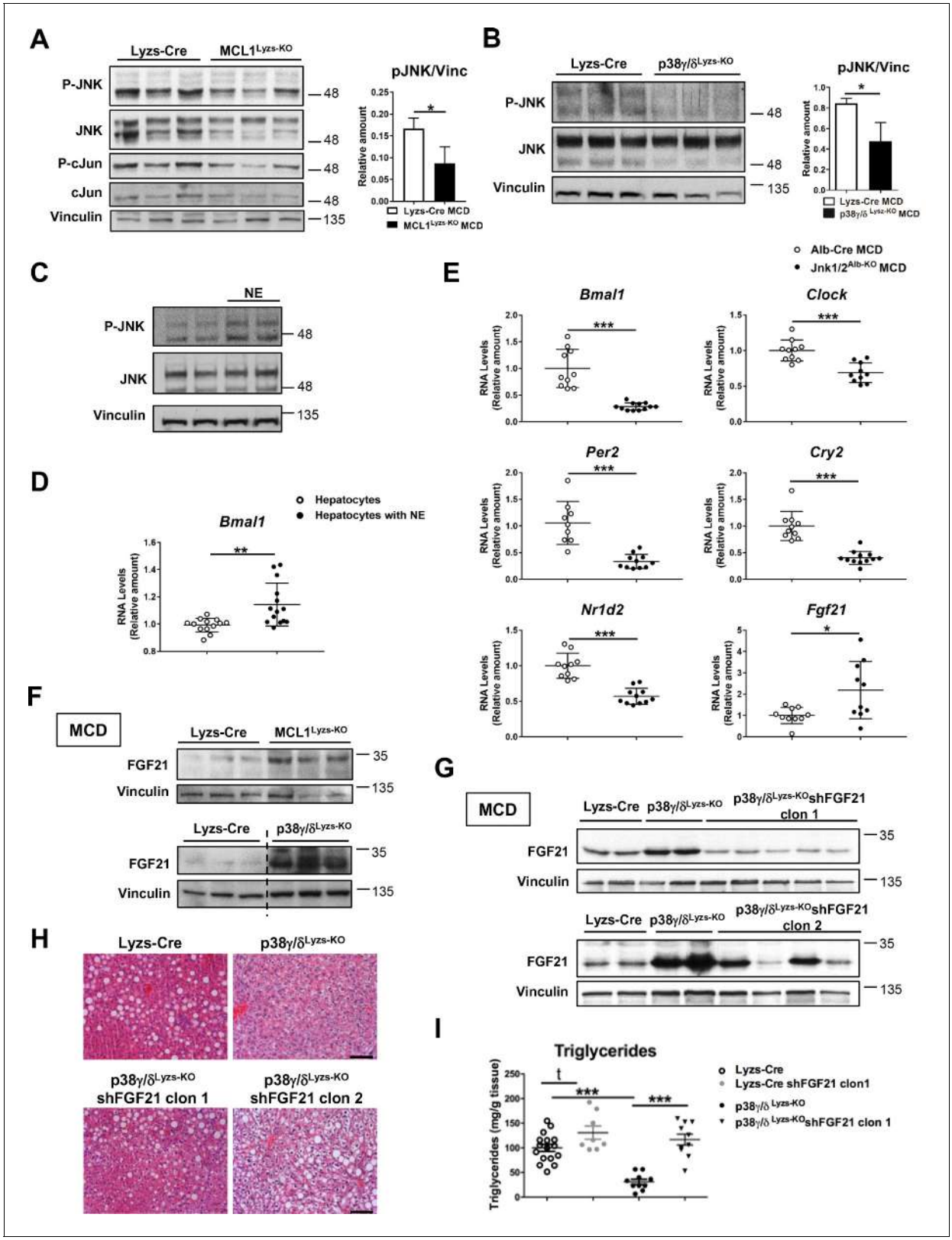

Figure 3. Diurnal regulation of liver metabolism involves neutrophil-mediated regulation of JNK and the hepatokine FGF21. Immunoblot analysis of JNK content and activation at ZT2 in liver extracts prepared from control (Lyzs-Cre) and neutropenic (MCL1$^{Lyzs-KO}$) mice fed a MCD diet for 3 weeks (**A**) or Lyzs-Cre and p38γ/δ$^{Lyzs-KO}$ mice after 3 weeks of MCD diet (**B**). Immunoblot analysis of JNK content and activation (**C**) and *Bmal1* RNA expression (**D**) in hepatocyte cultures exposed to NE for 2 hr (n = 14 wells of 3 independent experiments). Immunoblot quantification is shown in ***Figure 3—figure***

Figure 3 continued on next page

Figure 3 continued

supplement 1D (**E**) qRT-PCR analysis of clock genes and *Fgf21* in livers from Alb-Cre, and JNK1/2$^{Alb\text{-}KO}$ mice after 3 weeks of MCD diet at ZT2 (n = 9-12). (**F**) Immunoblot analysis of FGF21 content in liver extracts prepared from control (Lyzs-Cre) and neutropenic (MCL1$^{Lyzs\text{-}KO}$) mice, or from Lyzs-Cre, and p38γ/δ$^{Lyzs\text{-}KO}$ mice after 3 weeks of MCD diet sacrificed at ZT2. Immunoblot quantification is shown in ***Figure 3—figure supplement 1I,J***. (**G–I**) Lyzs-Cre and p38γ/δ$^{Lyzs\text{-}KO}$ mice were injected with 2 shRNA independent clones targeting FGF21. Seven days after infection, mice were placed on the MCD diet and sacrificed after 3 weeks at ZT2. (**G**) Immunoblot analysis of FGF21 content in liver extracts prepared from Lyzs-Cre, p38γ/δ$^{Lyzs\text{-}KO}$, and p38γ/δ$^{Lyzs\text{-}KO}$ mice infected with FGF21 shRNA. Immunoblot quantification is shown in ***Figure 3—figure supplement 1K***. (**H**) Representative H&E-stained liver sections. Scale bar, 50 μm. (**I**) Hepatic triglyceride content at the end of the treatment period (n = 8-10). Data are means ± SEM from at least 2 independent experiments. *p<0.05; **p<0.01; ***p<0.005 (**A, B, D and E**) *t*-test or Welch's test. (**I**) One-way ANOVA with Bonferroni post hoc test or *t-test*.

The online version of this article includes the following source data and figure supplement(s) for figure 3:

Source data 1. Raw data and statistical test.
Figure supplement 1. Neutrophils regulate hepatic metabolism and clock genes through JNK and FGF21.
Figure supplement 1—source data 1. Raw data and statistical test.

Cry2 expression, compared to control mice (***Figure 4B***), which mimicked the behavior of neutropenic mice. In addition, NE$^{-/-}$ mice presented lower respiratory quotient during the lights-on period than WT mice, indicating that these mice have increased fat utilization as a source of energy (***Figure 4C***), supporting the data that reduced liver-neutrophil infiltration results in higher lipid oxidation. Interestingly, when fed MCD or HFD diet, NE$^{-/-}$ mice were protected against steatosis (***Figure 4D,E*** and ***Figure 4—figure supplement 1A,B***), presented lower JNK activation, and expressed less ACC than control mice (***Figure 4F,G*** and ***Figure 4—figure supplement 1D***). Besides, NE$^{-/-}$ mice were protected against alterations in clock-gene expression induced by MCD diet, presenting lower expression of *Bmal1* and higher of *Cry2* and *Per2* comparing to control mice at ZT2 (***Figure 4H***). Furthermore, under HFD, NE$^{-/-}$ mice were also refractory to these changes as these mice maintained a pattern of clock-gene expression similar to control mice in ND (***Figure 4—figure supplement 1E***).

To formally test a direct contribution of NE in the regulation of hepatic clock-gene expression and liver metabolism, we infused WT or NE$^{-/-}$ neutrophils into neutropenic mice under the jet lag protocol (***Figure 5A***). The infusion of WT neutrophils was able to increase *Bmal1* expression in the liver after jet lag, while neutropenic mice infused with NE$^{-/-}$ neutrophils presented the same levels of *Bmal1* than non-infused neutropenic mice (***Figure 5B***). In addition, while infusion of neutropenic mice with WT neutrophils increased steatosis, neutropenic mice infused with NE$^{-/-}$ neutrophils presented the same levels of steatosis than control neutropenic mice (***Figure 5C,D***). All these data indicate that diet or jet-lag -induced hepatic infiltration of neutrophils results in dysregulation of the liver clock, and the lack of NE is enough to protect mice against these alterations.

Finally, to evaluate the translational relevance of these findings for human physiology we quantified in human livers the expression levels for the genes encoding NE, *JUN* (as an indicator of JNK activation) and Bmal. Our results suggest that the levels of *ELANE* expression directly correlate with *BMAL1* and *JUN* mRNA in livers from a human cohort (***Figure 5E***). These correlations reinforce the idea that a rhythmic neutrophil infiltration in the liver controls the expression of clock genes through the JNK pathway activation and could be a target for therapeutic intervention during non-alcoholic fatty liver disease.

Discussion

Our analysis demonstrates that neutrophils control clock genes in the liver and that reduced neutrophil infiltration protects against jet lag and diet-induced liver steatosis by altering the expression of these temporal regulators. These findings establish neutrophils as unexpected players in the regulation of daily hepatic metabolism. Our results also demonstrate that at least part of this neutrophil-induced clock modulation is mediated by elastase. These results agree with previous data showing that NE mediates the deleterious effects of neutrophils on liver metabolism and that mice lacking NE are protected against diet-induced steatosis (***Mansuy-Aubert et al., 2013***; ***Talukdar et al., 2012***). The molecular mechanism underlying this regulation involves neutrophil NE that induces activation of JNK and consequently inhibits the production of the hepatokine FGF21. The JNK pathway

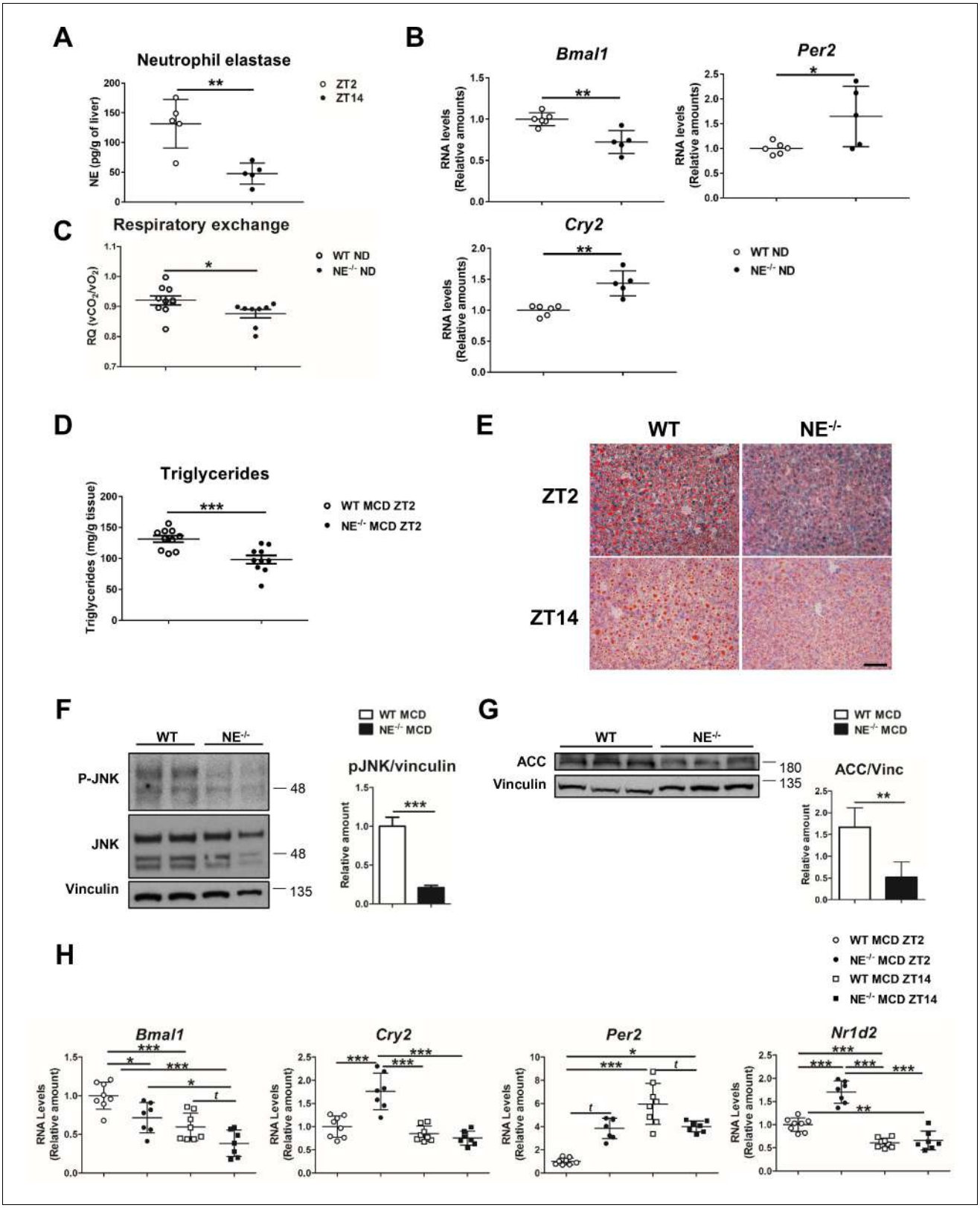

Figure 4. Elastase controls liver clock-gene expression modulating JNK activation. (**A**) Extracellular NE levels in livers from WT mice at ZT2 and ZT14. (**B**) qRT-PCR analysis of clock-genes and nuclear-receptor mRNA expression in livers from WT and NE KO mice ($NE^{-/-}$) at ZT2 (n = 5–6). (**C**) Respiratory exchange ratio of WT and $NE^{-/-}$ mice fed with ND. Results are from the lights-on period (n = 9). (**D–H**) WT and $NE^{-/-}$ mice were fed a MCD diet for 3 weeks and sacrificed at the indicated time. (**D**) Liver triglycerides at the end of the diet period. (**E**) Representative oil-red-stained liver sections. Scale

Figure 4 continued on next page

Figure 4 continued

bar, 50 μm (n = 10). (**F**) Immunoblot analysis and quantifications of JNK content and activation in liver extracts prepared from WT and $NE^{-/-}$. (**G**) Immunoblot analysis and quantification of ACC content in liver extracts from WT and $NE^{-/-}$ mice. (**H**) qRT-PCR analysis of clock-genes and nuclear-receptor mRNA expression in livers from WT and $NE^{-/-}$ mice at ZT2 and ZT14 (n = 7–8). Data are means ± SEM from at least two independent experiments. *p<0.05; **p<0.01; ***p<0.005 (A to G) *t*-test or Welch's test. (**H**) One-way ANOVA with to Tukey's post hoc test, *t-test* or Welch's test.
The online version of this article includes the following source data and figure supplement(s) for figure 4:

Source data 1. Raw data and statistical test.
Figure supplement 1. Neutrophil elastase regulates daily hepatic metabolism through JNK.

is an important modulator of liver metabolism, and lack of JNK1 and JNK2 in hepatocytes protects against steatosis (***Manieri and Sabio, 2015***). Here, we also demonstrate that JNK also regulates hepatocyte clock genes and, therefore, modulates diurnal adaptation of liver metabolism.

Recently published data have demonstrated that lipogenesis is increased in the light phase, in agreement with our analysis (***Guan et al., 2018***). We show that neutrophil infiltration causes JNK activation down-stream of elastase secretion, a time-dependent process. Indeed, phosphoproteomic analysis of the hepatic phosphorylation network identifies JNK as a key signaling enzyme with peak activation at ZT6 (***Robles et al., 2017***) immediately prior to the peak of lipogenic gene expression (***Guan et al., 2018***). Our results suggest that neutrophils induce an accumulative activation of JNK with a peak during the day that would control the lipogenic program.

Recent evidence established that the metabolic effects of JNK in the liver are mediated by FGF21 (***Vernia et al., 2016***; ***Vernia et al., 2014***). Our results now show that liver FGF21 expression can be modulated through the control of JNK by neutrophils. Reduction of FGF21 by shRNA reverted the protective effect and metabolic changes induced by reduced neutrophil infiltration. In conclusion, our results show that the diurnal oscillating migratory properties of neutrophils regulate liver function in a manner that preserves daily metabolic rhythms, and that disturbance of this rhythmicity can cause disease. These results might imply a novel mechanism of action for the potential use of clock-modulating small molecules in liver health.

Materials and methods

Study population

For the analysis of human liver mRNA levels, individuals were recruited among patients who underwent laparoscopic cholecystectomy for gallstone disease. The study was approved by the Ethics Committee of the University Hospital of Salamanca (Spain), and all subjects provided written informed consent to participate. Patients were excluded if they had a history of alcohol use disorders or excessive alcohol consumption, chronic hepatitis C or B, or body mass index $\geq$35. Baseline characteristics of these groups are listed in ***Figure 5—source data 1***.

Animal models

Neutropenic mice were generated with MCL1 (B6.129-Mcl1tm3Sjk/J) crossed with B6.Cg-Tg (S100A8-Cre,-EGFP)1Ilw/J mice or B6.129P2-Lyz2tm1(cre)Ifo/J mice. Mice deficient in NE, with compound JNK1/2 deficiency in hepatocytes, with Cxcr2 deficiency in neutrophils or with *p38γ/δ* deficiency in myeloid compartment have been described (***Belaaouaj et al., 1998***; ***Das et al., 2011***; ***Das et al., 2009***; ***González-Terán et al., 2016***) All mice were backcrossed for 10 generations to the C57BL/6J background (Jackson Laboratory). Genotypes were confirmed by PCR analysis of genomic DNA.

Mice were housed under a 12 hr light:12 hr dark cycle (Light is on at Zeitgeber Time ZT0 and off at ZT12). For jet lag experiments, the 12 hr:12 hr dark/light cycle was disrupted by extending the dark cycle 12 hr every 5 days over 3 weeks (***Kettner et al., 2016***). $Cxcr2^{MRP8\text{-}KO}$ chimeras were generated by exposing WT recipient mice to 2 doses of ionizing radiation (625 Gy) and reconstituting them with 5×10^6 donor BM ($Cxcr2^{MRP8\text{-}KO}$) cells injected into the tail vein.

Mice were fed a methionine-choline-deficient (MCD) diet for 3 weeks or a high-fat diet (HFD) for 8 weeks (Research Diets Inc). For neutrophil depletion, mice mini-osmotic pumps (Alzet) were implanted with anti-Ly6G antibody or saline (0.4 mg/kg per day, 21 days). For JNK inhibition

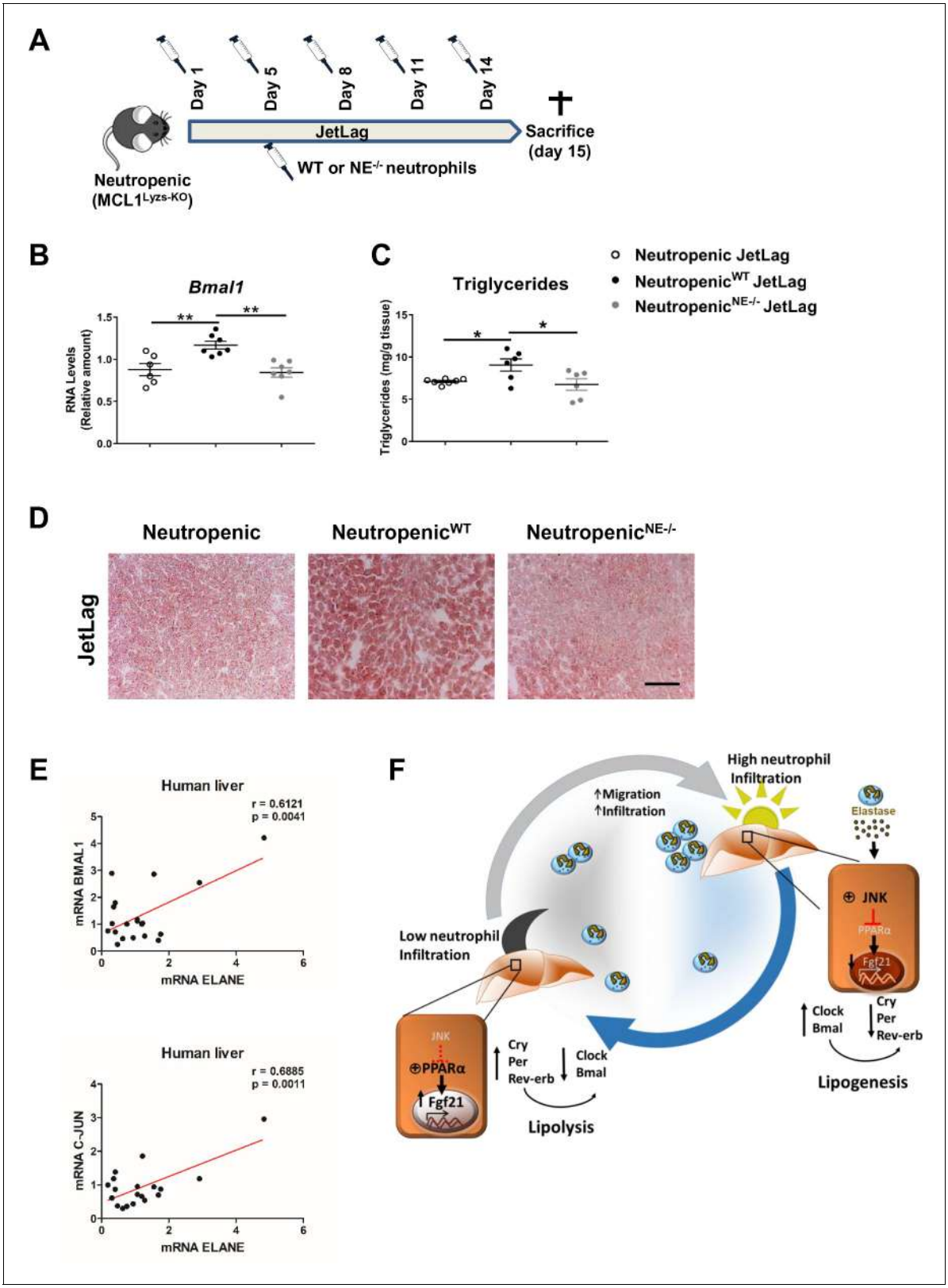

Figure 5. Neutrophil elastase reverses neutropenic mice phenotype through regulation of daily hepatic metabolism. (**A–D**) Neutropenic (MCL1$^{Lyzs\text{-}KO}$) mice were housed for 2 weeks with the dark period extended by 12 hr every 5 days (JetLag). Mice were infused with purified WT or NE$^{-/-}$ neutrophils. Samples were obtained at ZT14. (**A**) Picture describing the neutrophil infusion schedule during the JetLag protocol. (**B**) qRT-PCR analysis of *Bmal1* mRNA in livers. (**C**) Liver triglycerides and (**D**) representative oil-red-stained liver sections. Scale bar, 50 μm (n = 6-7). Data are means ± SEM. *p<0.05;

Figure 5 continued on next page

Figure 5 continued

t-test. (**E**) Correlation between mRNA levels of *BMAL1* and *ELANE* (r = 0.6141; p = 0.0052) or *JUN* and *ELANE* (r = 0.7362; p = 0.001105) in human livers. The mRNA levels of *JUN*, *BMAL1* and *ELANE* were determined by qRT-PCR. Linear relationships between variables were tested using Pearson's correlation coefficient (n = 23). (**F**) Circadian neutrophil infiltration regulates hepatic metabolism through elastase, JNK and FGF21. Data are means ± SEM. *p< 0.05; **p< 0.01; (B) One-way ANOVA with Tukey's pots hoc test. (**C**) *t-test* or Welch's test.
The online version of this article includes the following source data for figure 5:

Source data 1. Baseline characteristics of the human cohort.

experiments, mice were intraperitoneally injected with SP600125 (15 mg/kg) (Santa Cruz Biotechnology) at ZT0. For neutrophil infusion experiments, mice were intravenously injected with 3×10^6 WT or $NE^{-/-}$ purified neutrophils each 3–4 days. Neutrophils were isolated from BM using biotinylated anti-Ly6G antibody (Clone:1A8) and streptavidin-labeled magnetic microbeads (Miltenyi Biotec).

All animal procedures conformed to EU Directive 86/609/EEC and Recommendation 2007/526/EC regarding the protection of animals used for experimental and other scientific purposes, enacted under Spanish law 1201/2005.

Cell cultures

Hepatocytes were isolated from adult females by collagenase liver perfusion and cells were filtered through a 70 µm strainer. Hepatocytes pelleted from centrifuged Percoll gradients were plated at 4×10^5 cells/well on 6-well plates coated with collagen type one and incubated at 37˚C. After 24 hr, cells were treated with 0.5 mM palmitate (Sigma-Aldrich) for 6 hr and then exposed for 1 hr to freshly neutrophils (2×10^6 cells/well) in the presence of 1 µM FMLP (Sigma-Aldrich). Neutrophils were isolated from BM as described above. For some experiments, neutrophils were sorted purified form the BM using an anti-Ly6G antibody (Clone: 1A8). T and B lymphocytes were sorted purified from spleens using anti-CD3 (Clone: 145–2 C11) and anti-B220 (Clone: RA3-6B2), and bone marrow macrophages (BMDM) were differentiated as previously described (***González-Terán et al., 2013***). All antibodies were purchased from BD Pharmingen. Alternatively, hepatocytes were exposed 2 hr to 5 nM NE (R and D Systems) or 0.5 mg/mL of collagenase A (Roche) after palmitate treatment.

Isolation of liver-infiltrating leukocytes

Mice were perfused with 20 mL of PBS and livers were collected and dissociated. Cell suspension was passed through a 70 µm strainer and centrifuged twice at 50 xg for 2 min to discard the liver parenchyma. For some experiments, livers were incubated for 15 min with 1 mg/mL Collagenase A (Roche) and 2 U/mL DNase (Sigma) at 37˚C, and lungs were incubated for 25 min with 0,25 mg/ml Liberase TL (Sigma) and 5 U/mL DNase (Sigma) at 37˚C Leukocyte fraction was collected and stained with anti-CD45 (Clone: 30-F11), from Invitrogen, anti-CD11b (Clone: M1/70), anti-Ly6G (Clone: 1A8) or anti-Ly6C/G (Clone: RB6-8C5), from BD Pharmingen, and alternatively, with anti-F4/80 (Clone: BM8), from Invitrogen, and Goat anti-Clec4F from R and D Systems and conjugated with anti-goat Alexa 647. Cells were sorted on a FACSAria to >95% purity. Flow cytometry experiments were performed with a FACScan cytofluorometer (FACS Canto BD), and data were analyzed with FlowJo software.

Lentivirus vector production

Transient calcium phosphate transfection of HEK-293 cells (#CRL-1573, ATCC) was performed with the pGIPZ empty or pGIPZ.shFGF21 vector (V3LMM_430499 and V3LMM_430501, from Dharmacon) together with pΔ8.9 and pVSV-G. The supernatants were collected, centrifuged (700 xg, 4˚C, 10 min) and concentrated (165x) by ultracentrifugation for 2 hr at 121,986 xg at 4˚C (Ultraclear Tubes, SW28 rotor and Optima L-100 XP Ultracentrifuge; Beckman). Mice received tail-vein injections of 200 µl of lentiviral particles.

RNA analysis

Expression of mRNA was examined by qRT-PCR using a 7900 Fast Real Time thermocycler and Fast Sybr Green assays (Applied Biosystems). Relative mRNA expression was normalized to *Gapdh* and *Actb* mRNA. The primers used were as follows: *Actb* (F: GGCTGTATTCCCCTCCATCG; R: CCAG

TTGGTAACAATGCCATGT); *Gapdh* (F: TGAAGCAGGCATCTGAGGG; R: CGAAGGTGGAAGAG TGGGA); *Clock* (F: AGAACTTGGCATTGAAGAGTCTC; R: GTCAGACCCAGAATCTTGGCT); *Bmal1* (F: TGACCCTCATGGAAGGTTAGAA; R: GGACATTGCATTGCATGTTGG); *Nr1d2* (F: CAGACACTTC TTAAAGCGGCACTG; R: GGAGTTCATGCTTGTGAAGGCTGT); *Cry2* (F: CACTGGTTCCGCAAAG-GACTA; R: CCACGGGTCGAGGATGTAG); *Per2* (F: GAAAGCTGTCACCACCATAGAA; R: AAC TCGCACTTCCTTTTCAGG); *Acaca* (F: GATGAACCATCTCCGTTGGC; R: GACCCAATTATGAA TCGGGAGTG); *Fgf21* (F: CTGCTGGGGGTCTACCAAG; R: CTGCGCCTACCACTGTTCC); *Mip1a* (F: TTCTCTGTACCATGACACTCTGC; R: CGTGGAATCTTCCGGCTGTAG); *Mip2* (F: CCAACCAC-CAGGCTACAGG; R: GCGTCACACTCAAGCTCTG); *KC* (F: CTGGGATTCACCTCAAGAACATC; R: CAGGGTCAAGGCAAGCCTC); *Sdf-1* (F: GCTCTGCATCAGTGACGGTA; R: ATCTGAAGGGCACAG TTTGG); *Elane* (F: ATTTCCGGTCAGTGCAGGTAGT; R: GGTCAAAGCCATTCTCGAAGAT); *GAPDH* (F: CCATGAGAAGTATGACAACAGCC; R: GGGTGCTAAGCAGTTGGTG); *ELANE* (F: TCCACGGAA TTGCCTCCTTC; R: CCTCGGAGCGTTGGATGATA); *BMAL1* (F: GCCGAATGATTGCTGAGG; R: CACTGGAAGGAATGTCTGG); *JUN* (F: GGATCAAGGCGGAGAGGAAG; R: GCGTTAGCATGAG TTGGCAC).

Measurement of hepatic triglycerides

Lipids were extracted from 25 mg of liver in isopropanol (50 mg/mL) and centrifuged (15 min 9500 xg 4˚C). Triglycerides were detected in the supernatant (Sigma-Aldrich).

Histology

Tissue samples were fixed in 10% formalin for 48 hr, dehydrated, and embedded in paraffin. Sections (5 µm) were cut and stained with hematoxylin and eosin (Sigma-Aldrich and Thermo Scientific). Sections (8 µm) from frozen tissue and embedded in OCT compound (Tissue-Tek) were stained with Oil Red O (American Master Tech Scientific). Sections were examined in Leica DM2500 microscope using 20x objective.

Immunoblotting

Tissue extracts were prepared in Triton lysis buffer [20 mM Tris (pH 7.4), 1% Triton X-100, 10% glycerol, 137 mM NaCl, 2 mM EDTA, 25 mM β-glycerophosphate, 1 mM sodium orthovanadate, 1 mM phenylmethylsulfonyl fluoride, and 10 µg/mL aprotinin and leupeptin]. Extracts (20–50 µg protein) were examined by immunoblot. The antibodies employed were anti-FGF21 (1/1000, #RD281108100, BioVendor), anti-phospho JNK (1/1000, #4668S, Cell Signaling), anti-JNK (1/1000, #9252S, Cell Signaling), anti-phospho c-Jun (1/1000, #9164L, Cell Signaling), anti-c-Jun (1/1000, #9165S, Cell Signaling), anti-ACC (1/1000, #3676S, Cell Signaling), and anti-vinculin (1/5000, #V9131, Sigma). Anti-phospho JNK and anti-JNK antibodies recognize the two different JNK isoform (JNK1 and JNK2) and their two spliced variants (JNK1 (46 kDa), JNK1 (54 kDa) and JNK2 (46 kDa) and JNK2 (54 kDa)). Immunocomplexes were detected by enhanced chemiluminescence (Amersham).

Immunofluorescence

For 3-D imaging, livers were fixed in a solution of paraformaldehyde 4% in PBS at 4˚C. After washing in PBS, tissues were stored overnight in 30% sucrose (Sigma) with PBS. Then, livers were embedded in OCT compound (Tissue-Tek) and frozen at −80˚C. Cryosections of organs (70 µm) were washed in PBS and blocked/permeabilized in PBS with 10% donkey serum (Millipore) and 1% Triton. Primary antibodies diluted in blocking/permeabilization buffer were incubated overnight at 4˚C, followed by three washes in PBS and 2 hr incubation with secondary antibodies and DAPI at room temperature. After three washes in PBS, cells were mounted with Fluoromount-G (SouthernBiotech). The following primary and secondary antibodies were used: rat anti-CD31 (1:200, #553370 BD Pharmingen,), rabbit anti-S100A9 (mrp14) (1:100, #AB242945, Abcam,), goat anti-Clec4f (1:100, #AF2784, RD System), Alexa 488 donkey anti rat IgG (1:200, #A-21208, ThermoFisher), Cy3 AffiniPure Fab Fragment Donkey Anti-Rabbit IgG (1:200, #711-167-003, Jackson Laboratories), Alexa Fluor 633 donkey anti goat IgG (H+L) (1:200, #A21082, ThermoFisher). Immunostaining were imaged with a SP8 confocal microscope using 40x objectives. Individual fields or tiles of large areas were acquired every 2.5 µm for a total of 30 µm in depth. 3D images were obtained with Fiji/ImageJ 3D Viewer plugging.

For 2-D imaging, liver sections (12 µm) prepared from frozen tissue and embedded in OCT compound were fixed with 2% paraformaldehyde and permeabilized with PBS 0.1% Triton. After blocking with PBS 5% BSA 0.1% Triton and washing, tissues were incubated overnight at 4˚C with primary antibody. Then, sections were washed and incubated with conjugated secondary antibodies for 1 hr at room temperature and nuclei were stained with Sytox Green (Invitrogen) after washing. The following primary and secondary antibodies were used: rat anti-mouse S100A9 (Mrp-14) antibody (1:200, #AB105472, Abcam), rabbit anti-Neutrophil Elastase antibody (1:200, #AB68672, Abcam), goat Alexa Fluor 405 anti-rabbit (1:200) and goat Alexa Fluor 568 anti-rat IgG (1:500). Sections were mounted in Vectashield mounting medium (Vector, H-1000) and examined using a Leica SP5 multiline inverted confocal microscope and 20x objectives.

NE measurement

20 mL of PBS prefunded livers were crushed with a syringe plunger, resuspended in 4 mL of PBS/EDTA 5 mM/0.5% FBS and filtered (70 µm). Cell suspension was centrifuged at 1800 rpm 5 min and the supernatant was filtered (22 µm). Supernatants were concentrated using Amicon Ultra centrifugal filters (Sigma-Aldrich). NE levels were determined with Mouse Neutrophil Elastase ELISA kit (R and D system).

Quantification and statistical analysis

All data are expressed as means ± SEM. For comparisons between two groups, the Student's *t*-test was applied. For data with more than two data sets, we used one-way ANOVA coupled with Turkey's multigroup test. When variances were unequal, Welch's test or Kruskal-Wallis test coupled with Dunn's multiple comparison test were applied, respectively. Multiple group comparisons in the rhythmicity of neutrophil infiltration were analyzed with two-way ANOVA followed by Fisher's *post hoc* test. Significance was determined as a 2-sided $p < 0.05$. All statistical analyses were conducted in GraphPad Prism software. Statistical details were indicated in the figure legends.

Acknowledgements

We thank S Bartlett for English editing. We are grateful to A Zychlinsky for the $NE^{-/-}$ mice. We thank the staff at the CNIC Genomics, Cellomics, Microscopy, and Bioinformatics units for technical support and help with data analysis. BGT and MC were fellows of the FPI: Severo Ochoa CNIC program (SVP-2013–067639) and (BES-2017–079711) respectively. IN was funded by EFSD/Lilly grants (2017 and 2019), the CNIC IPP FP7 Marie Curie Programme (PCOFUND-2012–600396), EFSD Rising Star award (2019), JDC-2018-Incorporación (MIN/JDC1802). T-L was a Juan de la Cierva fellow (JCI-2011–11623). C.F has a Sara Borrell contract (CD19/00078). RJD is an Investigator of the Howard Hughes Medical Institute. This work was funded by the following grants to GS: funding from the European Union's Seventh Framework Programme (FP7/2007-2013) under grant agreement n˚ ERC 260464, EFSD/Lilly European Diabetes Research Programme Dr Sabio, 2017 Leonardo Grant for Researchers and Cultural Creators, BBVA Foundation (Investigadores-BBVA-2017) IN[17]_BBM_BAS_0066, MINECO-FEDER SAF2016-79126-R and PID2019-104399RB-I00 , EUIN2017-85875, Comunidad de Madrid IMMUNOTHERCAN-CM S2010/BMD-2326 and B2017/BMD-3733 and Fundación AECC AECC PROYE19047SABI and AECC: INVES20026LEIV to ML. MM was funded by ISCIII and FEDER PI16/01548 and Junta de Castilla y León GRS 1362/A/16 and INT/M/17/17 and JL-T by Junta de Castilla y León GRS 1356/A/16 and GRS 1587/A/17. The study was additionally funded by MEIC grants to ML (MINECO-FEDER-SAF2015-74112-JIN) AT-L (MINECO-FEDER-SAF2014-61233-JIN), RJD: Grant DK R01 DK107220 from the National Institutes of Health. AH: (SAF2015-65607-R). The CNIC is supported by the Instituto de Salud Carlos III (ISCIII), the Ministerio de Ciencia, Innovación y Universidades (MCNU) and the Pro CNIC Foundation, and is a Severo Ochoa Center of Excellence (SEV-2015–0505).

Additional information

Funding

Funder	Grant reference number	Author
European Commission	ERC260464	Guadalupe Sabio
Ministerio de Economía y Competitividad	SAF2016-79126-R	Guadalupe Sabio
Ministerio de Economía y Competitividad	SAF2015-74112-JIN	Magdalena Leiva
Fundación Científica Asociación Española Contra el Cáncer	INVES20026LEIV PROYE19047SABI	Magdalena Leiva Guadalupe Sabio
Ministerio de Ciencia e Innovación	PID2019-104399RB-I00	Guadalupe Sabio
FPI Severo Ochoa- CNIC	SVP-2013-067639	Barbara Gonzalez-Teran
Ministerio de Economía y Competitividad	BES-2017-079711	María Crespo
Juan de la Cierva	JCI-2011-11623	Antonia Tomás-Loba
Sara Borrell	CD19/00078	Cintia Folgueira
National Institutes of Health	DK R01 DK107220	Roger J Davis
Ministerio de Economía y Competitividad	SAF2014-61233-JIN	Antonia Tomás-Loba
Fundación BBVA	IN[17]_BBM_BAS_0066	Guadalupe Sabio
Ministerio de Economía y Competitividad	EUIN2017-85875	Guadalupe Sabio
Comunidad de Madrid	S2010/BMD-2326	Guadalupe Sabio
Comunidad de Madrid	B2017/BMD-3733	Guadalupe Sabio
Instituto de Salud Carlos III	PI16/01548	Miguel Marcos
Junta de Castilla y León	GRS1362/A/16	Miguel Marcos
Junta de Castilla y León	INT/M/17/17	Miguel Marcos
Junta de Castilla y León	GRS 1356/A/16	Jorge L Torres
Junta de Castilla y León	GRS 1587/A/17	Jorge L Torres
European Foundation for the Study of Diabetes	ESFD/Lilly Programme	Guadalupe Sabio
European Foundation for the Study of Diabetes	EFSD/Lilly Grant 2017 and 2019	Ivana Nikolic
CNIC IPP FP7 Marie Curie Programme	PCOFUND-2012-600396	Ivana Nikolic
European Foundation for the Study of Diabetes	EFSD Rising Star award 2019	Ivana Nikolic
Juan de la Cierva	JDC-2018-Incorporación MIN/JDC1802	Ivana Nikolic

The funders had no role in study design, data collection and interpretation, or the decision to submit the work for publication.

Author contributions

María Crespo, Barbara Gonzalez-Teran, Data curation, Formal analysis, Investigation, Methodology, Writing - review and editing; Ivana Nikolic, Cintia Folgueira, Macarena Fernández-Chacón, Antonia Tomás-Loba, Noelia A-Gonzalez, Daniel Beiroa, Formal analysis, Investigation, Methodology; Alfonso Mora, Formal analysis, Investigation, Methodology, Writing - review and editing; Elena

Rodríguez, Luis Leiva-Vega, Aránzazu Pintor-Chocano, Ainoa Caballero-Molano, Lourdes Hernández-Cosido, Jorge L Torres, Norman J Kennedy, Roger J Davis, Rui Benedito, Miguel Marcos, Ruben Nogueiras, Andrés Hidalgo, Formal analysis, Methodology; Irene Ruiz-Garrido, Beatriz Cicuéndez, Data curation, Methodology; Nuria Matesanz, Magdalena Leiva, Conceptualization, Data curation, Formal analysis, Supervision, Investigation, Methodology, Writing - original draft, Writing - review and editing; Guadalupe Sabio, Conceptualization, Data curation, Supervision, Funding acquisition, Investigation, Methodology, Writing - original draft, Project administration, Writing - review and editing

Author ORCIDs
María Crespo https://orcid.org/0000-0003-3666-3415
Barbara Gonzalez-Teran https://orcid.org/0000-0002-4336-8644
Alfonso Mora https://orcid.org/0000-0002-6397-4836
Noelia A-Gonzalez http://orcid.org/0000-0003-0533-5216
Roger J Davis http://orcid.org/0000-0002-0130-1652
Magdalena Leiva https://orcid.org/0000-0001-7735-2459
Guadalupe Sabio https://orcid.org/0000-0002-2822-0625

Ethics
Human subjects: The study was approved by the Ethics Committee of the University Hospital of Salamanca (Spain), and all subjects provided written informed consent to participate.
Animal experimentation: All animal procedures conformed to EU Directive 86/609/EEC and Recommendation 2007/526/EC regarding the protection of animals used for experimental and other scientific purposes, enacted under Spanish law 1201/2005.

Decision letter and Author response
Decision letter https://doi.org/10.7554/eLife.59258.sa1
Author response https://doi.org/10.7554/eLife.59258.sa2

Additional files
Supplementary files
- Transparent reporting form

Data availability
All data generated or analysed during this study are included in the manuscript and supporting files.

References
Adrover JM, Del Fresno C, Crainiciuc G, Cuartero MI, Casanova-Acebes M, Weiss LA, Huerga-Encabo H, Silvestre-Roig C, Rossaint J, Cossío I, Lechuga-Vieco AV, García-Prieto J, Gómez-Parrizas M, Quintana JA, Ballesteros I, Martin-Salamanca S, Aroca-Crevillen A, Chong SZ, Evrard M, Balabanian K, et al. 2019. A neutrophil timer coordinates immune defense and vascular protection. *Immunity* **50**:390–402. DOI: https://doi.org/10.1016/j.immuni.2019.01.002, PMID: 30709741

Belaaouaj A, McCarthy R, Baumann M, Gao Z, Ley TJ, Abraham SN, Shapiro SD. 1998. Mice lacking neutrophil elastase reveal impaired host defense against gram negative bacterial Sepsis. *Nature Medicine* **4**:615–618. DOI: https://doi.org/10.1038/nm0598-615, PMID: 9585238

Casanova-Acebes M, Pitaval C, Weiss LA, Nombela-Arrieta C, Chèvre R, A-González N, Kunisaki Y, Zhang D, van Rooijen N, Silberstein LE, Weber C, Nagasawa T, Frenette PS, Castrillo A, Hidalgo A. 2013. Rhythmic modulation of the hematopoietic niche through neutrophil clearance. *Cell* **153**:1025–1035. DOI: https://doi.org/10.1016/j.cell.2013.04.040, PMID: 23706740

Casanova-Acebes M, Nicolás-Ávila JA, Li JL, García-Silva S, Balachander A, Rubio-Ponce A, Weiss LA, Adrover JM, Burrows K, A-González N, Ballesteros I, Devi S, Quintana JA, Crainiciuc G, Leiva M, Gunzer M, Weber C, Nagasawa T, Soehnlein O, Merad M, et al. 2018. Neutrophils instruct homeostatic and pathological states in naive tissues. *The Journal of Experimental Medicine* **215**:2778–2795. DOI: https://doi.org/10.1084/jem.20181468, PMID: 30282719

Das M, Sabio G, Jiang F, Rincón M, Flavell RA, Davis RJ. 2009. Induction of hepatitis by JNK-mediated expression of TNF-alpha. *Cell* **136**:249–260. DOI: https://doi.org/10.1016/j.cell.2008.11.017, PMID: 19167327

Das M, Garlick DS, Greiner DL, Davis RJ. 2011. The role of JNK in the development of hepatocellular carcinoma. *Genes & Development* **25**:634–645. DOI: https://doi.org/10.1101/gad.1989311, PMID: 21406557

Delezie J, Dumont S, Dardente H, Oudart H, Gréchez-Cassiau A, Klosen P, Teboul M, Delaunay F, Pévet P, Challet E. 2012. The nuclear receptor REV-ERBα is required for the daily balance of carbohydrate and lipid metabolism. *The FASEB Journal* **26**:3321–3335. DOI: https://doi.org/10.1096/fj.12-208751, PMID: 22562834

Dibner C, Schibler U, Albrecht U. 2010. The mammalian circadian timing system: organization and coordination of central and peripheral clocks. *Annual Review of Physiology* **72**:517–549. DOI: https://doi.org/10.1146/annurev-physiol-021909-135821, PMID: 20148687

Druzd D, Scheiermann C. 2013. Immunology. Some monocytes got rhythm. *Science* **341**:1462–1464. DOI: https://doi.org/10.1126/science.1244445, PMID: 24072913

Dzhagalov I, St John A, He YW. 2007. The antiapoptotic protein Mcl-1 is essential for the survival of neutrophils but not macrophages. *Blood* **109**:1620–1626. DOI: https://doi.org/10.1182/blood-2006-03-013771, PMID: 17062731

Eash KJ, Greenbaum AM, Gopalan PK, Link DC. 2010. CXCR2 and CXCR4 antagonistically regulate neutrophil trafficking from murine bone marrow. *The Journal of Clinical Investigation* **120**:2423–2431. DOI: https://doi.org/10.1172/JCI41649, PMID: 20516641

Fisher FM, Maratos-Flier E. 2013. Stress heats up the adipocyte. *Nature Medicine* **19**:17–18. DOI: https://doi.org/10.1038/nm.3058, PMID: 23296001

González-Terán B, Cortés JR, Manieri E, Matesanz N, Verdugo Á, Rodríguez ME, González-Rodríguez Á, Valverde ÁM, Valverde Á, Martín P, Davis RJ, Sabio G. 2013. Eukaryotic elongation factor 2 controls TNF-α translation in LPS-induced hepatitis. *Journal of Clinical Investigation* **123**:164–178. DOI: https://doi.org/10.1172/JCI65124, PMID: 23202732

González-Terán B, Matesanz N, Nikolic I, Verdugo MA, Sreeramkumar V, Hernández-Cosido L, Mora A, Crainiciuc G, Sáiz ML, Bernardo E, Leiva-Vega L, Rodríguez E, Bondía V, Torres JL, Perez-Sieira S, Ortega L, Cuenda A, Sanchez-Madrid F, Nogueiras R, Hidalgo A, et al. 2016. p38γ and p38δ reprogram liver metabolism by modulating neutrophil infiltration. *The EMBO Journal* **35**:536–552. DOI: https://doi.org/10.15252/embj.201591857, PMID: 26843485

Guan D, Xiong Y, Borck PC, Jang C, Doulias PT, Papazyan R, Fang B, Jiang C, Zhang Y, Briggs ER, Hu W, Steger D, Ischiropoulos H, Rabinowitz JD, Lazar MA. 2018. Diet-Induced circadian enhancer remodeling synchronizes opposing hepatic lipid metabolic processes. *Cell* **174**:831–842. DOI: https://doi.org/10.1016/j.cell.2018.06.031, PMID: 30057115

Haus E, Halberg F. 1966. Persisting circadian rhythm in hepatic glycogen of mice during inanition and dehydration. *Experientia* **22**:113–114. DOI: https://doi.org/10.1007/BF01900185, PMID: 5927958

Haus E, Smolensky MH. 1999. Biologic rhythms in the immune system. *Chronobiology International* **16**:581–622. DOI: https://doi.org/10.3109/07420529908998730, PMID: 10513884

He W, Holtkamp S, Hergenhan SM, Kraus K, de Juan A, Weber J, Bradfield P, Grenier JMP, Pelletier J, Druzd D, Chen CS, Ince LM, Bierschenk S, Pick R, Sperandio M, Aurrand-Lions M, Scheiermann C. 2018. Circadian expression of migratory factors establishes Lineage-Specific signatures that guide the homing of leukocyte subsets to tissues. *Immunity* **49**:1175–1190. DOI: https://doi.org/10.1016/j.immuni.2018.10.007, PMID: 30527911

Huang W, Ramsey KM, Marcheva B, Bass J. 2011. Circadian rhythms, sleep, and metabolism. *Journal of Clinical Investigation* **121**:2133–2141. DOI: https://doi.org/10.1172/JCI46043, PMID: 21633182

Keller M, Mazuch J, Abraham U, Eom GD, Herzog ED, Volk HD, Kramer A, Maier B. 2009. A circadian clock in macrophages controls inflammatory immune responses. *PNAS* **106**:21407–21412. DOI: https://doi.org/10.1073/pnas.0906361106, PMID: 19955445

Kettner NM, Voicu H, Finegold MJ, Coarfa C, Sreekumar A, Putluri N, Katchy CA, Lee C, Moore DD, Fu L. 2016. Circadian homeostasis of liver metabolism suppresses hepatocarcinogenesis. *Cancer Cell* **30**:909–924. DOI: https://doi.org/10.1016/j.ccell.2016.10.007, PMID: 27889186

Kohsaka A, Laposky AD, Ramsey KM, Estrada C, Joshu C, Kobayashi Y, Turek FW, Bass J. 2007. High-fat diet disrupts behavioral and molecular circadian rhythms in mice. *Cell Metabolism* **6**:414–421. DOI: https://doi.org/10.1016/j.cmet.2007.09.006, PMID: 17983587

Kolla BP, Auger RR. 2011. Jet lag and shift work sleep disorders: how to help reset the internal clock. *Cleveland Clinic Journal of Medicine* **78**:675–684. DOI: https://doi.org/10.3949/ccjm.78a.10083, PMID: 21968474

Kudo T, Kawashima M, Tamagawa T, Shibata S. 2008. *Clock* mutation facilitates accumulation of cholesterol in the liver of mice fed a cholesterol and/or cholic acid diet. *American Journal of Physiology-Endocrinology and Metabolism* **294**:E120–E130. DOI: https://doi.org/10.1152/ajpendo.00061.2007, PMID: 17971517

Lamia KA, Storch KF, Weitz CJ. 2008. Physiological significance of a peripheral tissue circadian clock. *PNAS* **105**:15172–15177. DOI: https://doi.org/10.1073/pnas.0806717105, PMID: 18779586

Li H, Zhang J, Jia W. 2013. Fibroblast growth factor 21: a novel metabolic regulator from pharmacology to physiology. *Frontiers of Medicine* **7**:25–30. DOI: https://doi.org/10.1007/s11684-013-0244-8, PMID: 23358894

Lucas D, Battista M, Shi PA, Isola L, Frenette PS. 2008. Mobilized hematopoietic stem cell yield depends on species-specific circadian timing. *Cell Stem Cell* **3**:364–366. DOI: https://doi.org/10.1016/j.stem.2008.09.004, PMID: 18940728

Manieri E, Sabio G. 2015. Stress kinases in the modulation of metabolism and energy balance. *Journal of Molecular Endocrinology* **55**:R11–R22. DOI: https://doi.org/10.1530/JME-15-0146, PMID: 26363062

Mansuy-Aubert V, Zhou QL, Xie X, Gong Z, Huang JY, Khan AR, Aubert G, Candelaria K, Thomas S, Shin DJ, Booth S, Baig SM, Bilal A, Hwang D, Zhang H, Lovell-Badge R, Smith SR, Awan FR, Jiang ZY. 2013. Imbalance between neutrophil elastase and its inhibitor α1-antitrypsin in obesity alters insulin sensitivity, inflammation, and energy expenditure. *Cell Metabolism* **17**:534–548. DOI: https://doi.org/10.1016/j.cmet.2013.03.005, PMID: 23562077

McNelis JC, Olefsky JM. 2014. Macrophages, immunity, and metabolic disease. *Immunity* **41**:36–48. DOI: https://doi.org/10.1016/j.immuni.2014.05.010, PMID: 25035952

Mei J, Liu Y, Dai N, Hoffmann C, Hudock KM, Zhang P, Guttentag SH, Kolls JK, Oliver PM, Bushman FD, Worthen GS. 2012. Cxcr2 and Cxcl5 regulate the IL-17/G-CSF axis and neutrophil homeostasis in mice. *The Journal of Clinical Investigation* **122**:974–986. DOI: https://doi.org/10.1172/JCI60588, PMID: 22326959

Méndez-Ferrer S, Lucas D, Battista M, Frenette PS. 2008. Haematopoietic stem cell release is regulated by circadian oscillations. *Nature* **452**:442–447. DOI: https://doi.org/10.1038/nature06685, PMID: 18256599

Nathan C. 2006. Neutrophils and immunity: challenges and opportunities. *Nature Reviews Immunology* **6**:173–182. DOI: https://doi.org/10.1038/nri1785, PMID: 16498448

North C, Feuers RJ, Scheving LE, Pauly JE, Tsai TH, Casciano DA. 1981. Circadian organization of thirteen liver and six brain enzymes of the mouse. *American Journal of Anatomy* **162**:183–199. DOI: https://doi.org/10.1002/aja.1001620302

Potthoff MJ, Kliewer SA, Mangelsdorf DJ. 2012. Endocrine fibroblast growth factors 15/19 and 21: from feast to famine. *Genes & Development* **26**:312–324. DOI: https://doi.org/10.1101/gad.184788.111, PMID: 22302876

Reppert SM, Weaver DR. 2002. Coordination of circadian timing in mammals. *Nature* **418**:935–941. DOI: https://doi.org/10.1038/nature00965, PMID: 12198538

Rey G, Cesbron F, Rougemont J, Reinke H, Brunner M, Naef F. 2011. Genome-wide and phase-specific DNA-binding rhythms of BMAL1 control circadian output functions in mouse liver. *PLOS Biology* **9**:e1000595. DOI: https://doi.org/10.1371/journal.pbio.1000595, PMID: 21364973

Robles MS, Cox J, Mann M. 2014. In-vivo quantitative proteomics reveals a key contribution of post-transcriptional mechanisms to the circadian regulation of liver metabolism. *PLOS Genetics* **10**:e1004047. DOI: https://doi.org/10.1371/journal.pgen.1004047, PMID: 24391516

Robles MS, Humphrey SJ, Mann M. 2017. Phosphorylation is a central mechanism for circadian control of metabolism and physiology. *Cell Metabolism* **25**:118–127. DOI: https://doi.org/10.1016/j.cmet.2016.10.004, PMID: 27818261

Scheiermann C, Kunisaki Y, Lucas D, Chow A, Jang JE, Zhang D, Hashimoto D, Merad M, Frenette PS. 2012. Adrenergic nerves govern circadian leukocyte recruitment to tissues. *Immunity* **37**:290–301. DOI: https://doi.org/10.1016/j.immuni.2012.05.021, PMID: 22863835

Solt LA, Wang Y, Banerjee S, Hughes T, Kojetin DJ, Lundasen T, Shin Y, Liu J, Cameron MD, Noel R, Yoo S-H, Takahashi JS, Butler AA, Kamenecka TM, Burris TP. 2012. Regulation of circadian behaviour and metabolism by synthetic REV-ERB agonists. *Nature* **485**:62–68. DOI: https://doi.org/10.1038/nature11030

Steimer DA, Boyd K, Takeuchi O, Fisher JK, Zambetti GP, Opferman JT. 2009. Selective roles for antiapoptotic MCL-1 during granulocyte development and macrophage effector function. *Blood* **113**:2805–2815. DOI: https://doi.org/10.1182/blood-2008-05-159145, PMID: 19064728

Su L, Li N, Tang H, Lou Z, Chong X, Zhang C, Su J, Dong X. 2018. Kupffer cell-derived TNF-α promotes hepatocytes to produce CXCL1 and mobilize neutrophils in response to necrotic cells. *Cell Death & Disease* **9**:323. DOI: https://doi.org/10.1038/s41419-018-0377-4, PMID: 29476069

Tahara Y, Shibata S. 2016. Circadian rhythms of liver physiology and disease: experimental and clinical evidence. *Nature Reviews Gastroenterology & Hepatology* **13**:217–226. DOI: https://doi.org/10.1038/nrgastro.2016.8, PMID: 26907879

Talukdar S, Oh DY, Bandyopadhyay G, Li D, Xu J, McNelis J, Lu M, Li P, Yan Q, Zhu Y, Ofrecio J, Lin M, Brenner MB, Olefsky JM. 2012. Neutrophils mediate insulin resistance in mice fed a high-fat diet through secreted elastase. *Nature Medicine* **18**:1407–1412. DOI: https://doi.org/10.1038/nm.2885, PMID: 22863787

Tiniakos DG, Vos MB, Brunt EM. 2010. Nonalcoholic fatty liver disease: pathology and pathogenesis. *Annual Review of Pathology: Mechanisms of Disease* **5**:145–171. DOI: https://doi.org/10.1146/annurev-pathol-121808-102132, PMID: 20078219

Toledo M, Batista-Gonzalez A, Merheb E, Aoun ML, Tarabra E, Feng D, Sarparanta J, Merlo P, Botrè F, Schwartz GJ, Pessin JE, Singh R. 2018. Autophagy Regulates the Liver Clock and Glucose Metabolism by Degrading CRY1. *Cell Metabolism* **28**:268–281. DOI: https://doi.org/10.1016/j.cmet.2018.05.023

Tong X, Yin L. 2013. Circadian rhythms in liver physiology and liver diseases. *Comprehensive Physiology* **3**:917–940. DOI: https://doi.org/10.1002/cphy.c120017, PMID: 23720334

Turek FW, Joshu C, Kohsaka A, Lin E, Ivanova G, McDearmon E, Laposky A, Losee-Olson S, Easton A, Jensen DR, Eckel RH, Takahashi JS, Bass J. 2005. Obesity and metabolic syndrome in circadian clock mutant mice. *Science* **308**:1043–1045. DOI: https://doi.org/10.1126/science.1108750, PMID: 15845877

Vernia S, Cavanagh-Kyros J, Garcia-Haro L, Sabio G, Barrett T, Jung DY, Kim JK, Xu J, Shulha HP, Garber M, Gao G, Davis RJ. 2014. The PPARα-FGF21 hormone Axis contributes to metabolic regulation by the hepatic JNK signaling pathway. *Cell Metabolism* **20**:512–525. DOI: https://doi.org/10.1016/j.cmet.2014.06.010, PMID: 25043817

Vernia S, Cavanagh-Kyros J, Barrett T, Tournier C, Davis RJ. 2016. Fibroblast growth factor 21 mediates glycemic regulation by hepatic JNK. *Cell Reports* **14**:2273–2280. DOI: https://doi.org/10.1016/j.celrep.2016.02.026, PMID: 26947074

Xu H, Li H, Woo S-L, Kim S-M, Shende VR, Neuendorff N, Guo X, Guo T, Qi T, Pei Y, Zhao Y, Hu X, Zhao J, Chen L, Chen L, Ji J-Y, Alaniz RC, Earnest DJ, Wu C. 2014. Myeloid Cell-specific Disruption of *Period1* and *Period2* Exacerbates Diet-induced Inflammation and Insulin Resistance. *Journal of Biological Chemistry* **289**:16374–16388. DOI: https://doi.org/10.1074/jbc.M113.539601

Yang X, Downes M, Yu RT, Bookout AL, He W, Straume M, Mangelsdorf DJ, Evans RM. 2006. Nuclear receptor expression links the circadian clock to metabolism. *Cell* **126**:801–810. DOI: https://doi.org/10.1016/j.cell.2006.06.050, PMID: 16923398

Zhang D, Tong X, Arthurs B, Guha A, Rui L, Kamath A, Inoki K, Yin L. 2014. Liver clock protein BMAL1 promotes *de* novo lipogenesis through insulin-mTORC2-AKT signaling. *Journal of Biological Chemistry* **289**:25925–25935. DOI: https://doi.org/10.1074/jbc.M114.567628, PMID: 25063808

Zhou P, Ross RA, Pywell CM, Liangpunsakul S, Duffield GE. 2015. Disturbances in the murine hepatic circadian clock in alcohol-induced hepatic steatosis. *Scientific Reports* **4**:3725. DOI: https://doi.org/10.1038/srep03725

Appendix 1

Appendix 1—key resources table

Reagent type (species) or resource	Designation	Source or reference	Identifiers	Additional information
Genetic reagent (*M. musculus*)	C57BL/6J background	Jackson Laboratory	Cat# 000664 RRID:IMSR_JAX:000664	
Genetic reagent (*M. musculus*)	B6.129-Mcl1tm3Sjk/J	Jackson Laboratory	Cat# 006088 RRID:IMSR_JAX:006088	
Genetic reagent (*M. musculus*)	B6.Cg-Tg(S100A8-cre,-EGFP)1Ilw/J	Jackson Laboratory	Cat# 021614 RRID:IMSR_JAX:021614	
Genetic reagent (*M. musculus*)	B6.129P2-Lyz2tm1(cre)Ifo/J	Jackson Laboratory	Cat# 004781 RRID:IMSR_JAX:004781	
Genetic reagent (*M. musculus*)	B6.129-Mapk12tm1.2	PMID:26843485		
Genetic reagent (*M. musculus*)	B6.129-Mapk13tm1.2	PMID:26843485		
Genetic reagent (*M. musculus*)	B6.129 × 1/SvJ-Elanetm1Sds	Jackson Laboratory	Cat# 006112 RRID:IMSR_JAX:006112	
Genetic reagent (*M. musculus*)	B6.Cg-Tg(Alb-cre)21Mgn/J	Jackson Laboratory	Cat# 003574 RRID:IMSR_JAX:003574	
Genetic reagent (*M. musculus*)	B6.129-Mapk8LoxP/LoxP Mapk9tm1Flv/J	PMID:19167327		
Genetic reagent (*M. musculus*)	C57BL/6-Cxcr2tm1Rmra/J	Jackson Laboratory	Cat# 024638 RRID:IMSR_JAX:024638	
Cell line (*H. sapiens*)	HEK-293	ATCC	Cat# CRL-1573 RRID:CVCL_0045	
Cell line (*M. musculus*)	Primary hepatocytes	PMID:26843485		
Transfected construct (synthesized)	pGIZP (pΔ8.9- pVSV-G)	Dharmacon	Cat# RHS4349	Lentiviral Empty Vector shRNA Control
Transfected construct (synthesized)	pGIZP.shFGF21 (pΔ8.9-pVSV-G)	Dharmacon	Cat# V3LMM_430499	
Transfected construct (synthesized)	pGIZP.shFGF21 (pΔ8.9-pVSV-G)	Dharmacon	Cat# V3LMM_430501	
Biological sample (*H. sapiens*)	Liver human samples	University Hospital of Salamanca-IBSAL	***Figure 5—source data 1***	
Antibody	Biotinylated monoclonal rat anti-mouse Ly6G (Clone 1A8)	Miltenyi Biotec	Cat# 130-123-854 RRID:AB_1036098	1:20
Antibody	Biotinylated monoclonal hamster anti-mouse CD3 (Clone 145–2 C11)	BD Pharmingen	Cat# 553057 RRID:AB_394590	1:20

Continued on next page

Appendix 1—key resources table continued

Reagent type (species) or resource	Designation	Source or reference	Identifiers	Additional information
Antibody	Biotinylated monoclonal rat anti-mouse B220 (Clone RA3-6B2)	BD Pharmingen	Cat# 561880 RRID:AB_10897020	1:20
Antibody	Monoclonal rat anti-mouse CD45 Pacific Orange (Clone 30-F11)	Invitrogen	Cat# MCD4530 RRID:AB_2539700	Flow cytometry 1:100
Antibody	Monoclonal rat anti-mouse CD11b FITC (Clone M1/70)	BD Pharmingen	Cat# 557396 RRID:AB_396679	Flow cytometry 1:100
Antibody	Monoclonal rat anti-mouse Ly6C/G APC (Clone RB6-8C5)	BD Pharmingen	Cat# 553129 RRID:AB_398532	Flow cytometry 1:200
Antibody	Monoclonal rat anti-mouse F4/80 PE-Cy7 (Clone BM8)	eBioscience	Cat# 25480182 RRID:AB_469653	Flow cytometry 1:100
Antibody	Monoclonal rat anti-Mouse Ly-6G PE (Clone 1A8)	BD Bioscience	Cat# 551461 RRID:AB_394208	Flow cytometry 1:200
Antibody	Polyclonal Chicken Anti Goat IgG (H+L) Alexa Fluor 647	Invitrogen	Cat# A-21469 RRID:AB_2535872	Flow cytometry 1:500
Antibody	Polyclonal rabbit anti-mouse FGF21	BioVendor	Cat# RD281108100 RRID:AB_2034054	WB 1:1000
Antibody	Monolconal rabbit anti-phospho SAPK/JNK (T183/Y185) (Clone 81E11)	Cell Signaling	Cat# 4668S RRID:AB_823588	WB 1:1000
Antibody	Polyclonal rabbit anti-SAPK/JNK	Cell Signaling	Cat# 9252S RRID:AB_2250373	WB 1:1000
Antibody	Polyclonal rabbit anti-phospho c-jun	Cell Signaling	Cat# 9164L RRID:AB_330892	WB 1:1000
Antibody	Monoclonal rabbit anti-c-jun (Clone 60A8)	Cell Signaling	Cat# 9165S RRID:AB_2130165	WB 1:1000
Antibody	Monoclonal rabbit anti-Acetyl-CoA carboxylase (Clone C83B10)	Cell Signaling	Cat# 3676S RRID:AB_2219397	WB 1:1000
Antibody	Monoclonal mouse anti-vinculin (Clone hVIN-1)	Sigma	Cat# V9131 RRID:AB_477629	WB 1:5000
Antibody	Polyclonal goat anti-Mouse IgG (H+L) Secondary Antibody, HRP	ThermoFisher	Cat# 31430 RRID:AB_228307	WB 1:5000
Antibody	Polyclonal goat anti-Rabbit IgG (H+L) Secondary Antibody, HRP	ThermoFisher	Cat# 31460 RRID:AB_228341	WB 1:5000
Antibody	Monoclonal rat anti-mouse CD31 (Clone MEC 13.3)	BD Pharmingen	Cat# 553370 RRID:AB_394816	IF 1:200

Continued on next page

Appendix 1—key resources table continued

Reagent type (species) or resource	Designation	Source or reference	Identifiers	Additional information
Antibody	Monoclonal rabbit anti-mouse S100A9 (mrp14) (Clone EPR22332-75)	Abcam	Cat# AB242945 RRID:AB_2876886	IF 1:100
Antibody	Polyclonal goat anti-mouse Clec4f	RD System	Cat# AF2784 RRID:AB_2081339	IF/Flow cytometry 1:200
Antibody	Polyclonal donkey anti rat IgG Alexa 488	ThermoFisher	Cat# A-21208 RRID:AB_2535794	IF 1:200
Antibody	Polyclonal Donkey Anti-Rabbit IgG Cy3 AffiniPure Fab Fragment	Jackson Laboratories	Cat# 711-167-003 RRID:AB_2340606	IF 1:200
Antibody	Polyclonal Donkey Anti Goat IgG (H+L) Alexa Fluor 633	ThermoFisher	Cat# A21082 RRID:AB_10562400	IF 1:200
Antibody	Monoclonal rat anti-mouse S100A9 (Mrp-14) (Clone 2B10)	Abcam	Cat# AB105472 RRID:AB_10862594	IF 1:200
Antibody	Polyclonal rabbit anti-neutrophil elastase	Abcam	Cat# AB68672 RRID:AB_1658868	IF 1:200
Antibody	Polyclonal goat Anti-Rabbit Alexa Fluor 405	ThermoFisher	Cat# A-31556 RRID:AB_221605	IF 1:200
Antibody	Polyclonal goat Anti-Rat IgG Alexa Fluor 568	ThermoFisher	Cat# A-11077 RRID:AB_2534121	IF 1:500
Sequence-based reagent	RT-qPCR primers	Sigma-Aldrich		
Peptide, recombinant protein	Recombinant Mouse Neutrophil Elastase/EL	R and D Systems	Cat# 4517-SE-010	
Peptide, recombinant protein	Collagenase A	Roche	Cat# 10 103 586 001	
Peptide, recombinant protein	Collagenase Type 1 CLS1	Worthington Biochemical	Cat# LS004197	
Peptide, recombinant protein	Liberase TL	Sigma	Cat# 5401020001	
Peptide, recombinant protein	DNase Type II-S	Sigma-Aldrich	Cat# D4513	
Commercial assay or kit	Serum Triglyceride Determination Kit	Sigma-Aldrich	Cat# TR0100-1KT	
Commercial assay or kit	Mouse Neutrophil Elastase/ ELA2 DuoSet ELISA	R and D systems	Cat# DY4517-05	
Commercial assay or kit	RNa easy Mini Kit	Qiagen	Cat# 74106	

Continued on next page

Appendix 1—key resources table continued

Reagent type (species) or resource	Designation	Source or reference	Identifiers	Additional information
Commercial assay or kit	High-Capacity cDNA Reverse Transcription Kit	Applied Biosystems	Cat# 4368814	
Chemical compound, drug	Fast SYBR Green Master Mix	Applied Biosystems	Cat# 4385616	
Chemical compound, drug	Percoll	GE Healthcare	Cat# 17-0891-01	
Chemical compound, drug	Palmitic acid	Sigma-Aldrich	Cat# P0500	
Chemical compound, drug	N-Formil Met-Leu-Phe (FMLP)	Sigma-Aldrich	Cat# F3506	
Chemical compound, drug	SP600125 (SAPK inhibitor)	Santa Cruz Biotechnology	Cat# sc-200635	
Chemical compound, drug	Amersham ECL Prime Western Blotting Detection Reagent	GE Healthcare	Cat# RPN2232	
Chemical compound, drug	Fluoromount-G	SouthernBiotech	Cat# 0100–01	
Chemical compound, drug	Sucrose	Sigma-Aldrich	Cat# S8501	
Chemical compound, drug	SYTOX Green Nucleic Acid Stain - 5 mM	ThermoFisher	Cat# S7020	
Chemical compound, drug	VECTASHIELD Antifade Mounting Medium	Vector Lab	Cat# H-1000	
Software, algorithm	GraphPad PRISM	GraphPad Software	RRID:SCR_002798	
Software, algorithm	Photoshop CS6	Adobe	RRID:SCR_014199	
Software, algorithm	Fiji/Image J software	Fiji-Image J	https://imagej.nih.gov/ij/ RRID:SCR_003070	
Software, algorithm	FlowJo	FlowJo	https://www.flowjo.com/ RRID:SCR_008520	
Software, algorithm	Leica LAS X	Leica Software	RRID:SCR_013673	
Other	Hematoxylin	Sigma	Cat# H3136	
Other	Eosin Y Alcoholic	Thermo Scientific	Cat# 6766008	
Other	OCT	Tissue-Tek	Cat# 4583	
Other	Oil Red O (C.I.26125)	American Master Tech Scientific	Cat# SPO1077	
Other	70 µM cell strainers	Corning Falcon	Cat# 352350	
Other	22 µM filter	Sigma-Aldrich	Cat# SLGPM33RS	
Other	Amicon Ultra centrifugal filters	Sigma-Aldrich	Cat# UFC800324	
Other	Magnetic streptavidin microbeads	Miltenyi Biotec	Cat# 130-048-101	

Continued on next page

Appendix 1—key resources table continued

Reagent type (species) or resource	Designation	Source or reference	Identifiers	Additional information
Other	MACS Separation Columns- MS columns	Miltenyi Biotec	Cat# 130-042-201	
Other	Mini-osmotic pumps	Alzet	Cat# 1004	
Other	Methionine-choline-deficient diet (MCD)	Research Diets Inc	Cat# A02082002B	
Other	High-fat diet (HFD)	Research Diets Inc	Cat# D11103002i	